# Light (anti)(hyper)nuclei production in Pb-Pb collisions measured with ALICE at the LHC

Ramona Lea
Dipartimento Di Fisica, Università di Trieste e INFN, Sezione Trieste
For the ALICE collaboration
20/05/2015

Strangeness in Nuclei and in Neutron Stars
20 – 21 May 2015 - Pisa

Introduction

Heavy ion collisions provide experimental access to the properties of nuclear matter under extreme conditions of temperature and density

Collective and thermal properties of the Quark Gluon Plasma can be inferred from transverse momentum (p_T) distributions and integrated yields of identified particles

Introduction

Heavy ion collisions provide experimental access to the properties of nuclear matter under extreme conditions of temperature and density

Collective and thermal properties of the Quark Gluon Plasma can be inferred from transverse momentum (p_T) distributions and integrated yields of identified particles

Time

Initial state

Hydrodynamic Evolution

Hadron Freeze-out
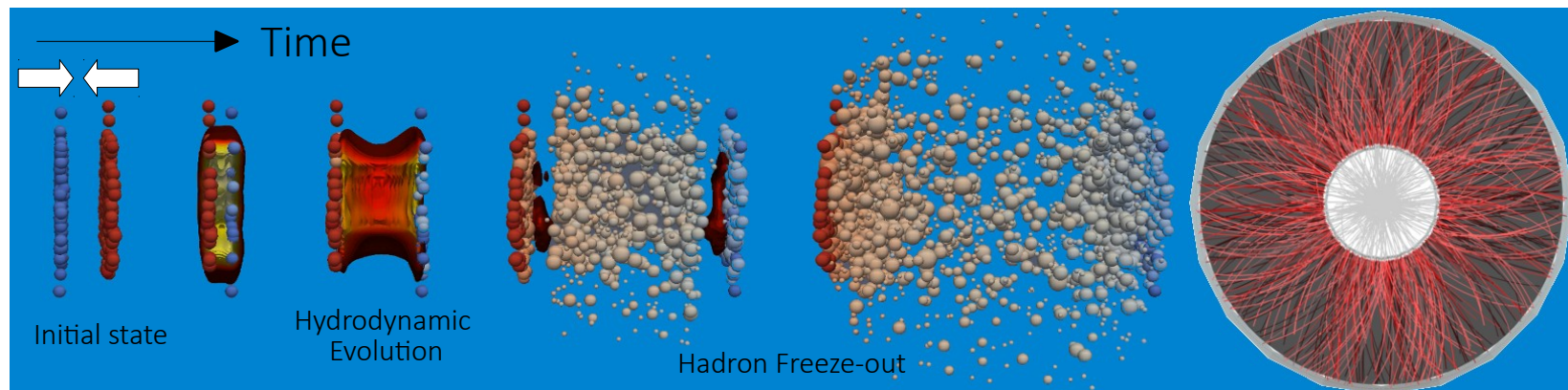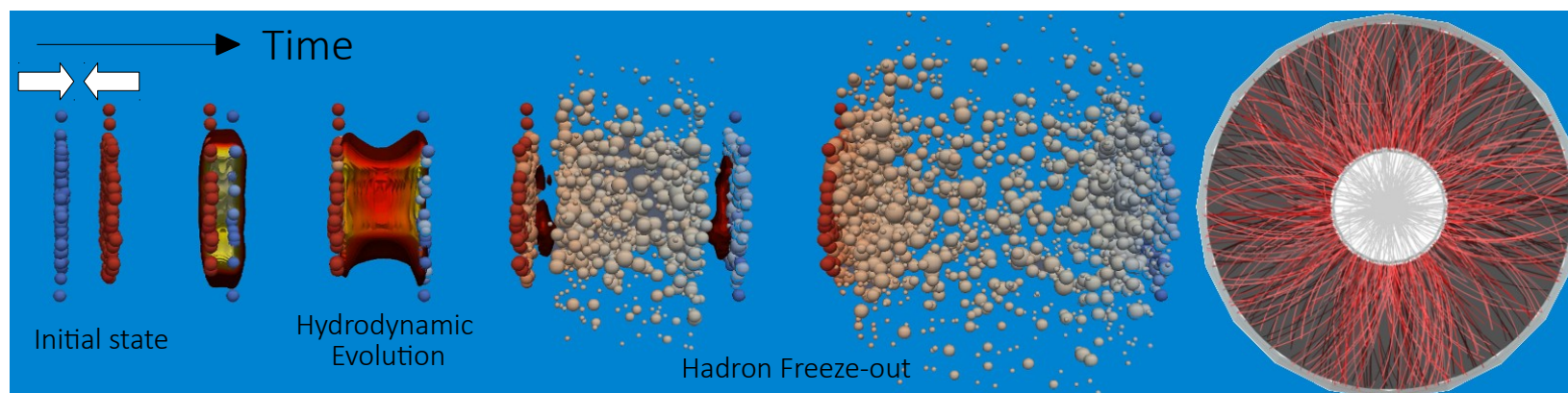
At LHC energies u$\bar{\text{u}}$, d$\bar{\text{d}}$, s$\bar{\text{s}}$ pairs can be easily excited from the quantum vacuum
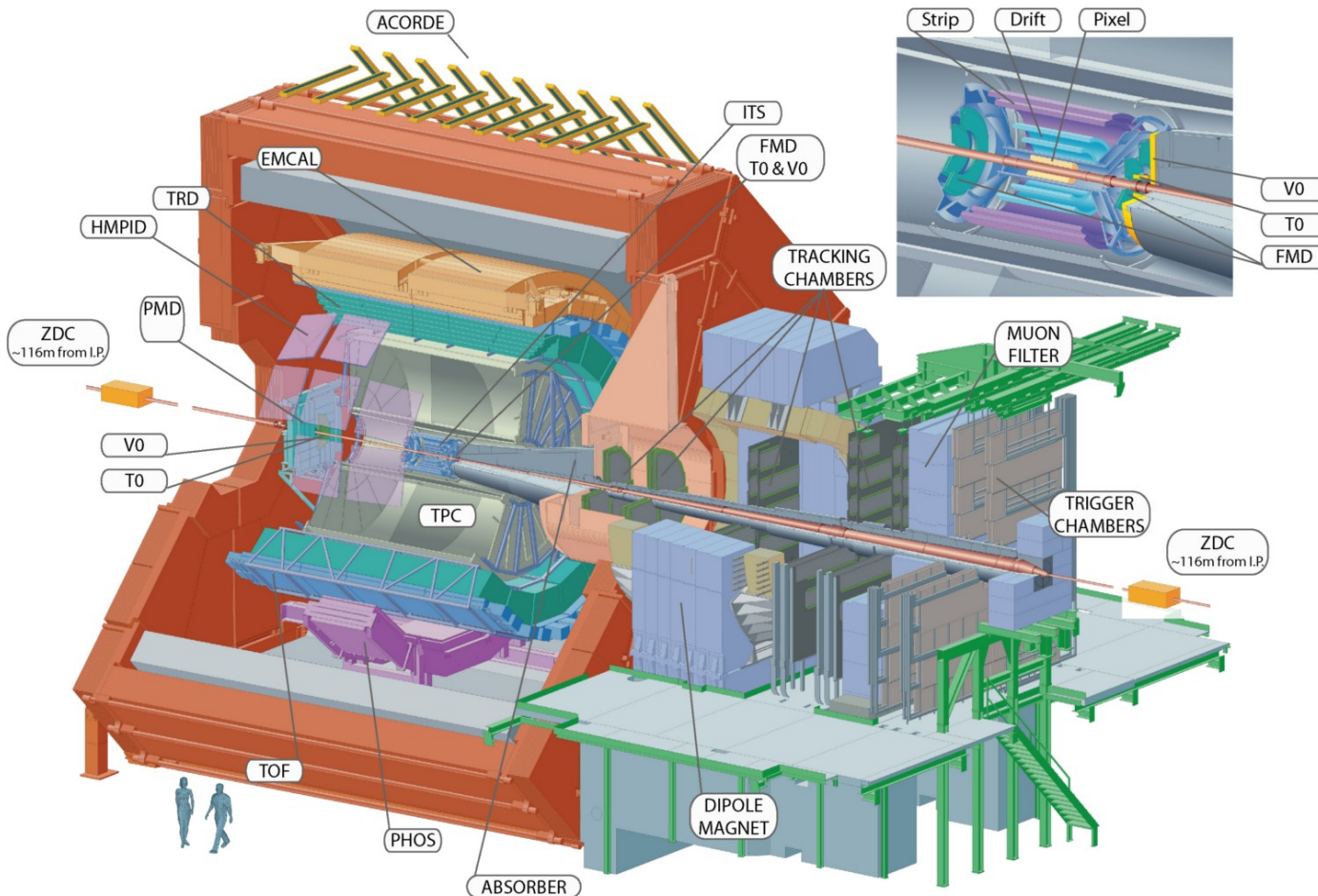 → abundant production of strangeness and antimatter

What can we learn from the measurement of (anti-)nuclei spectra and hyper-nuclei?
- Compare the results to expectations from thermal-statistical and from coalescence models
  → Investigate the late evolution of the fireball in heavy-ion collisions
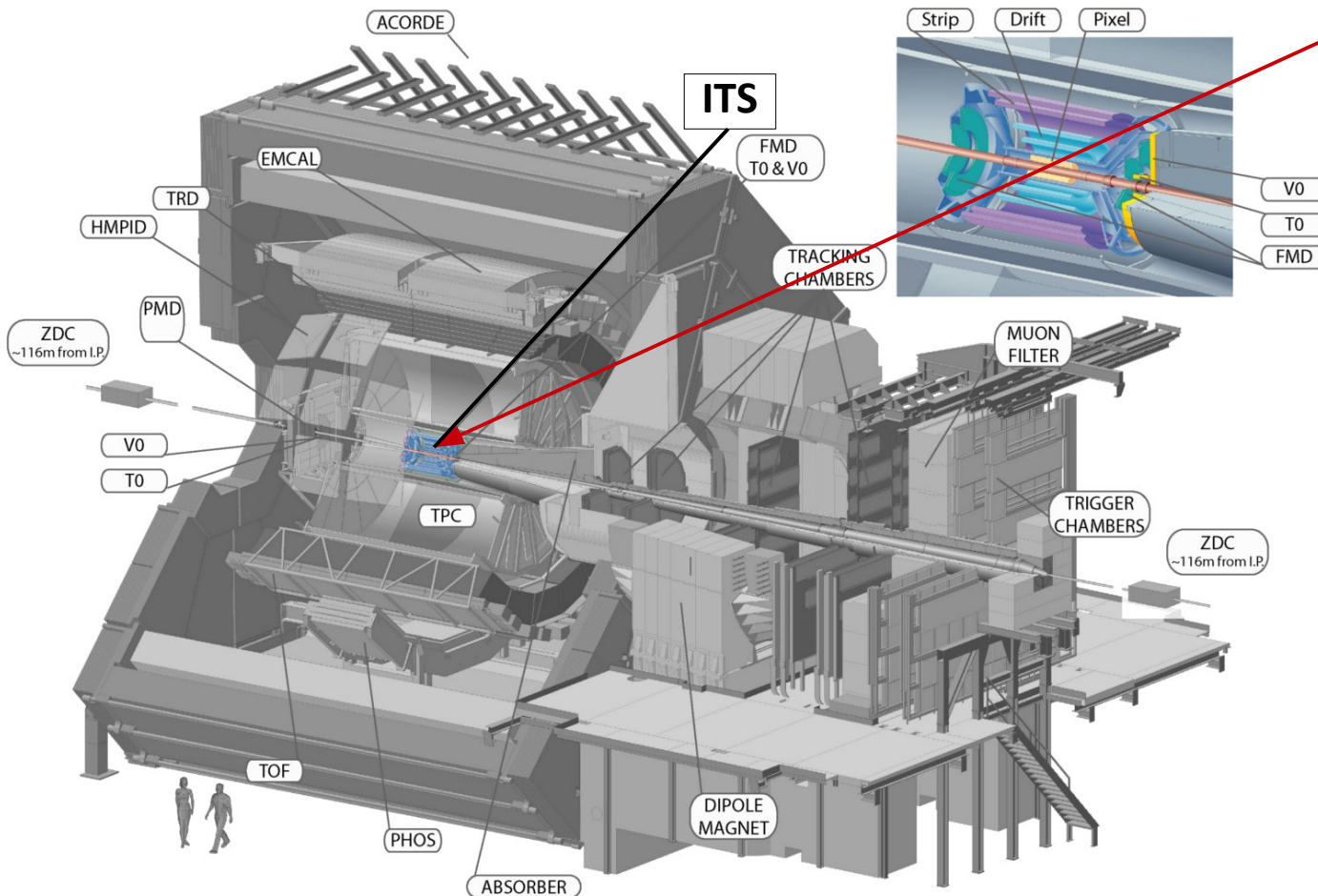- Baseline for searches for exotic bound states such as the H-Dibaryon and a Λn bound state

A Large Ion Collider Experiment

ALICE particle identification capabilities are unique. Almost all known techniques are exploited: dE/dx, Time Of Flight, Transition Radiation, Cherenkov Radiation, calorimetry and decay topology (V0, cascade).
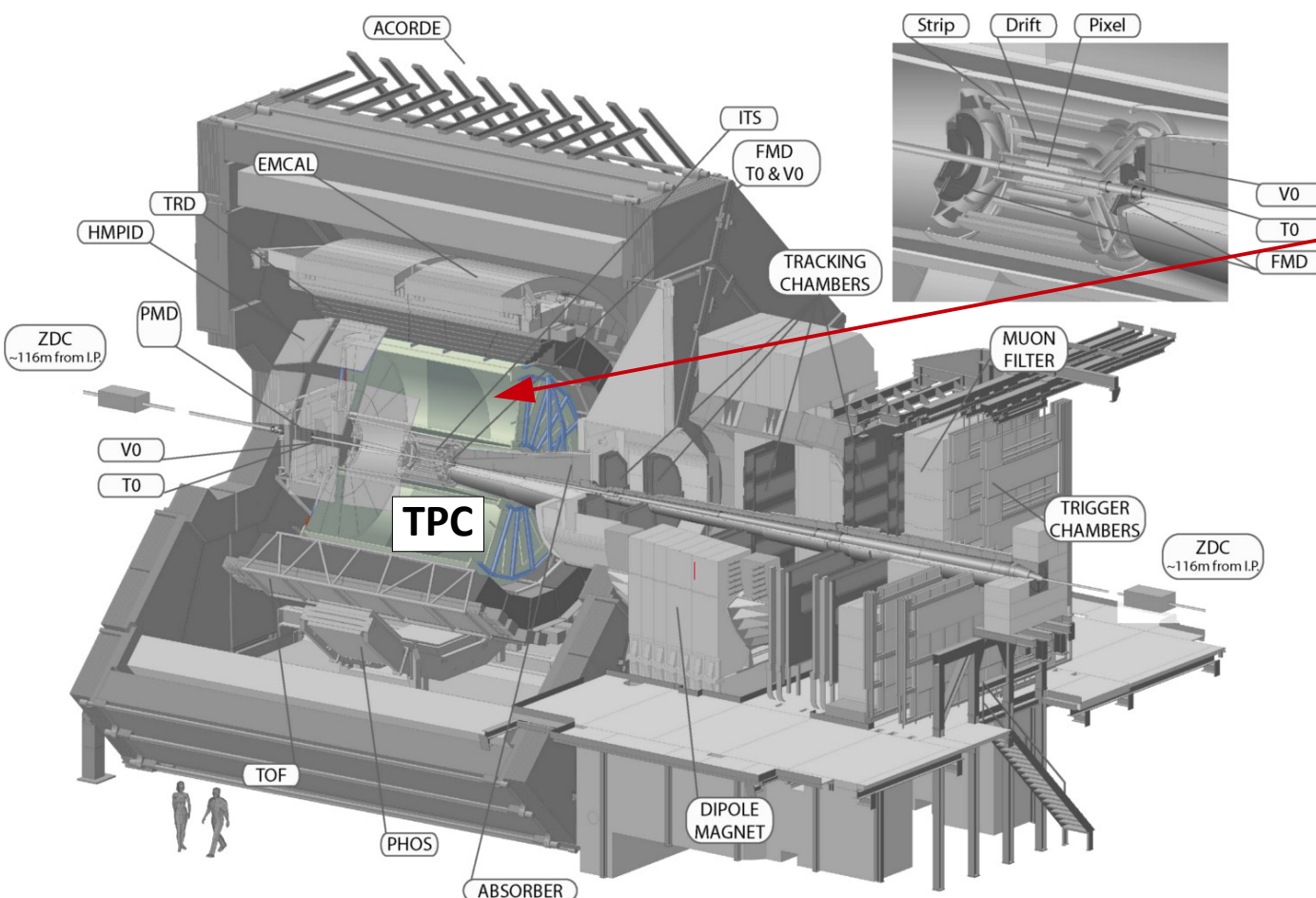
A Large Ion Collider Experiment

ALICE particle identification capabilities are unique. Almost all known techniques are exploited: dE/dx, Time Of Flight, Transition Radiation, Cherenkov Radiation, calorimetry and decay topology (V0, cascade).

Inner Tracking System (ITS) :
- Primary vertex
- Tracking
- Particle identification via dE/dx

A Large Ion Collider Experiment

ALICE particle identification capabilities are unique. Almost all known techniques are exploited: dE/dx, Time Of Flight, Transition Radiation, Cherenkov Radiation, calorimetry and decay topology (V0, cascade).

Inner Tracking System (ITS) :
- Primary vertex
- Tracking
- Particle identification via dE/dx

Time Projection Chamber (TPC):
- Global tracking
- Particle identification via dE/dx

A Large Ion Collider Experiment
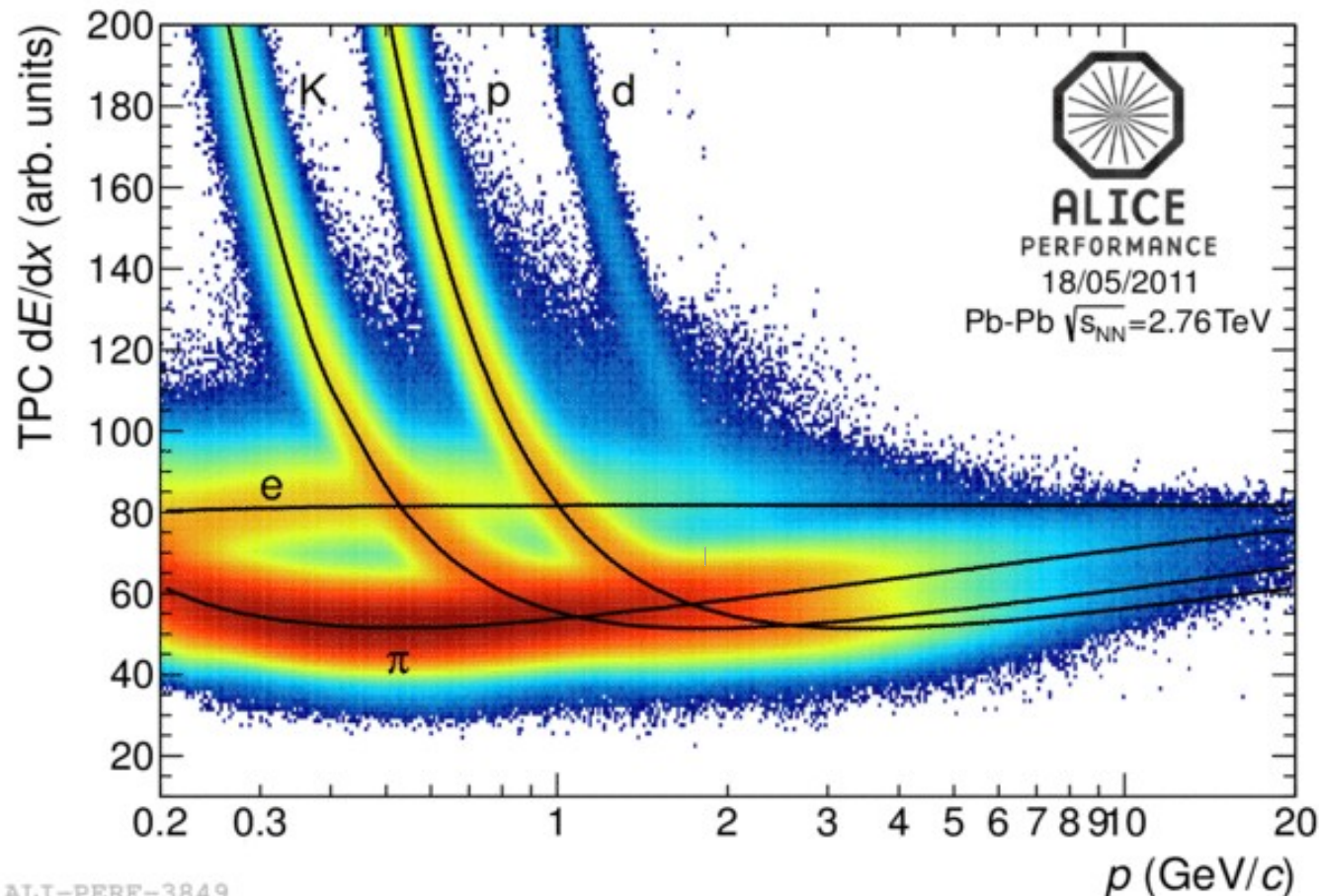
ALICE particle identification capabilities are unique. Almost all known techniques are exploited: dE/dx, Time Of Flight, Transition Radiation, Cherenkov Radiation, calorimetry and decay topology (V0, cascade).

Inner Tracking System (ITS) :
- Primary vertex
- Tracking
- Particle identification via dE/dx

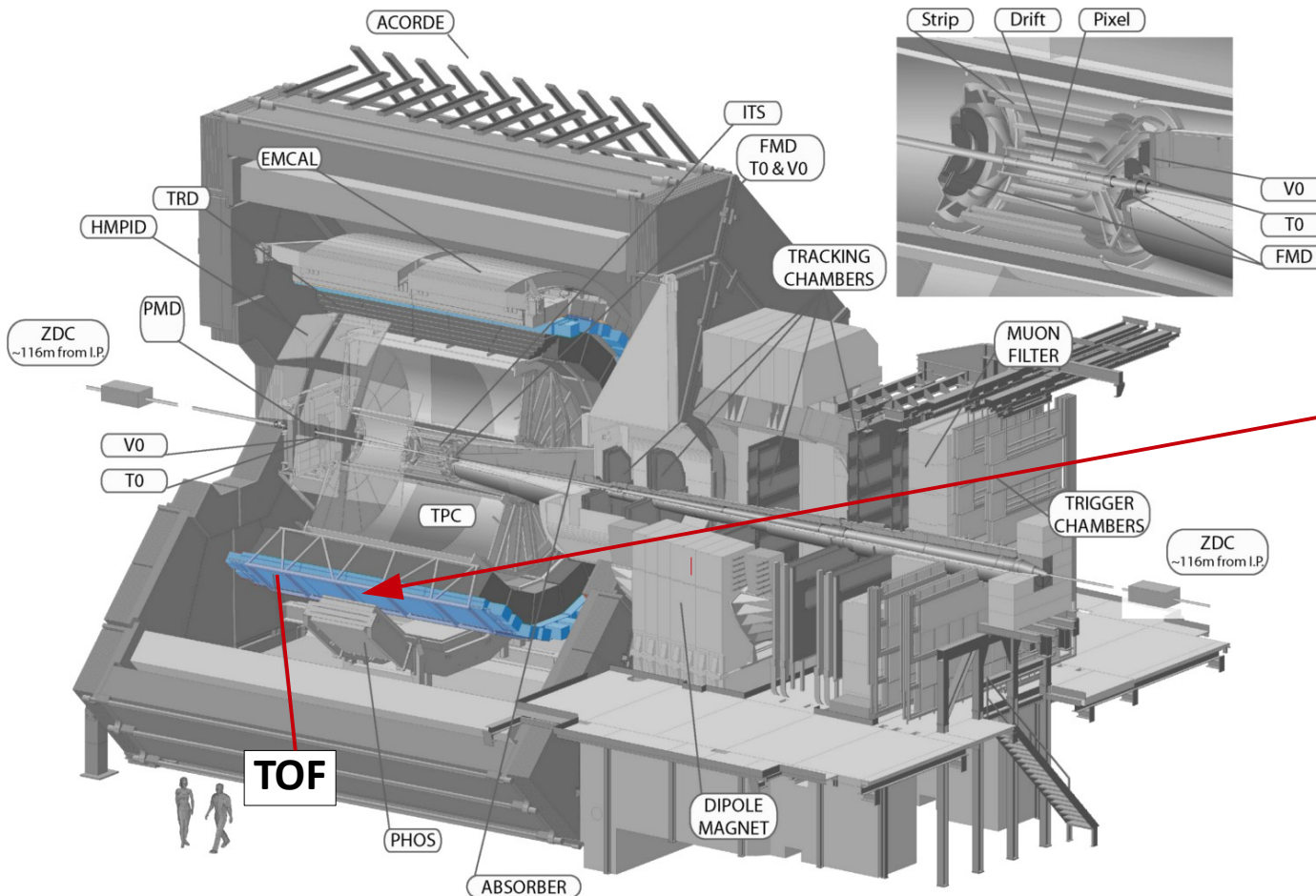**Time Projection Chamber (TPC):**
- Global tracking
- Particle identification via dE/dx

A Large Ion Collider Experiment

ALICE particle identification capabilities are unique. Almost all known techniques are exploited: dE/dx, Time Of Flight, Transition Radiation, Cherenkov Radiation, calorimetry and decay topology (V0, cascade).

Inner Tracking System (ITS) :
- Primary vertex
- Tracking
- Particle identification via dE/dx

Time Projection Chamber (TPC):
- Global tracking
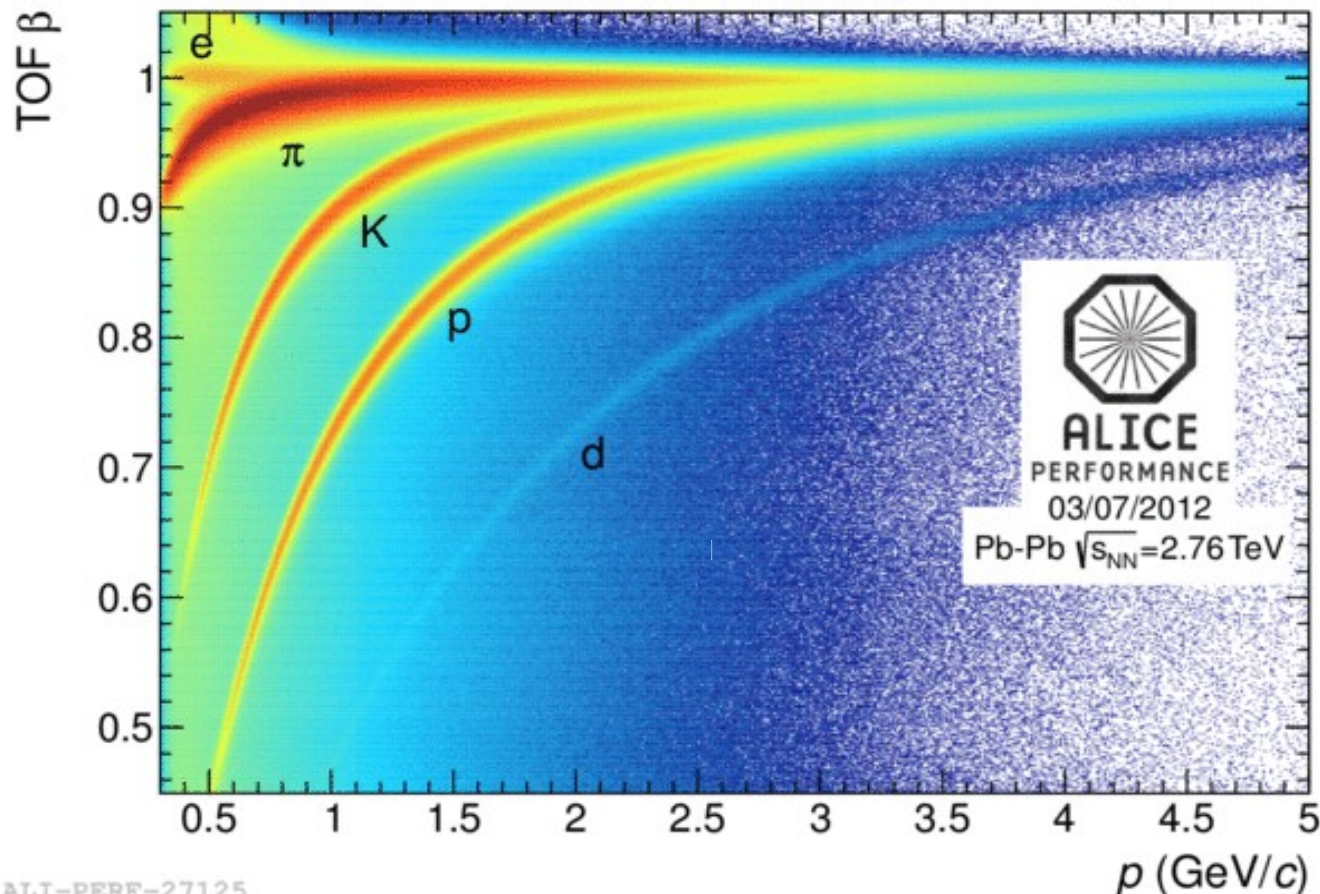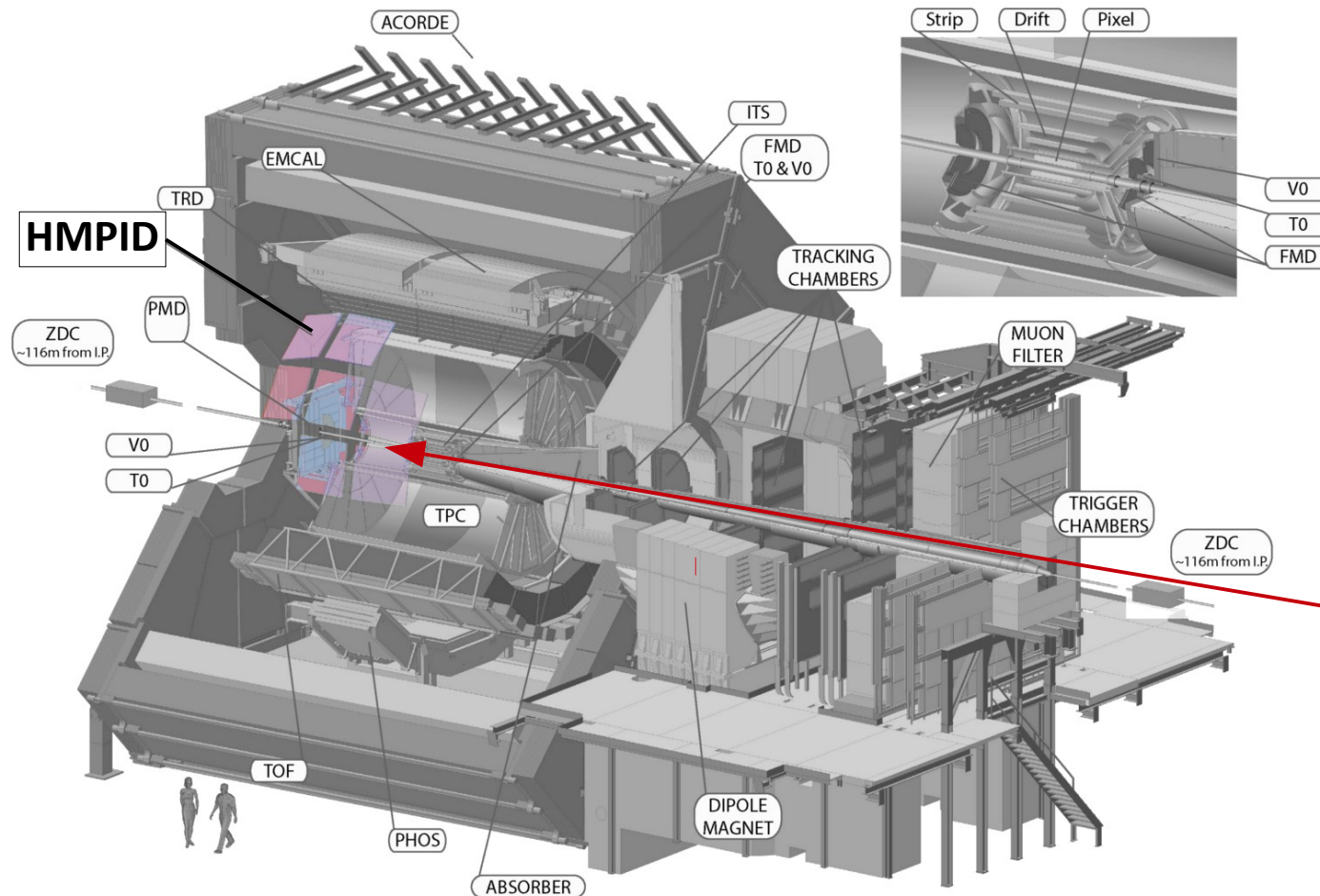- Particle identification via dE/dx

Time Of Flight (TOF):
- Particle identification via velocity measurement

A Large Ion Collider Experiment

ALICE particle identification capabilities are unique. Almost all known techniques are exploited: dE/dx, Time Of Flight, Transition Radiation, Cherenkov Radiation, calorimetry and decay topology (V0, cascade).

Inner Tracking System (ITS) :
- Primary vertex
- Tracking
- Particle identification via dE/dx

Time Projection Chamber (TPC):
- Global tracking
- Particle identification via dE/dx

Time Of Flight (TOF):
- Particle identification via velocity measurement

ALI-PERF-27125

A Large Ion Collider Experiment

ALICE particle identification capabilities are unique. Almost all known techniques are exploited: dE/dx, Time Of Flight, Transition Radiation, Cherenkov Radiation, calorimetry and decay topology (V0, cascade).

Inner Tracking System (ITS) :
- Primary vertex
- Tracking
- Particle identification via dE/dx

Time Projection Chamber (TPC):
- Global tracking
- Particle identification via dE/dx

Time Of Flight (TOF):
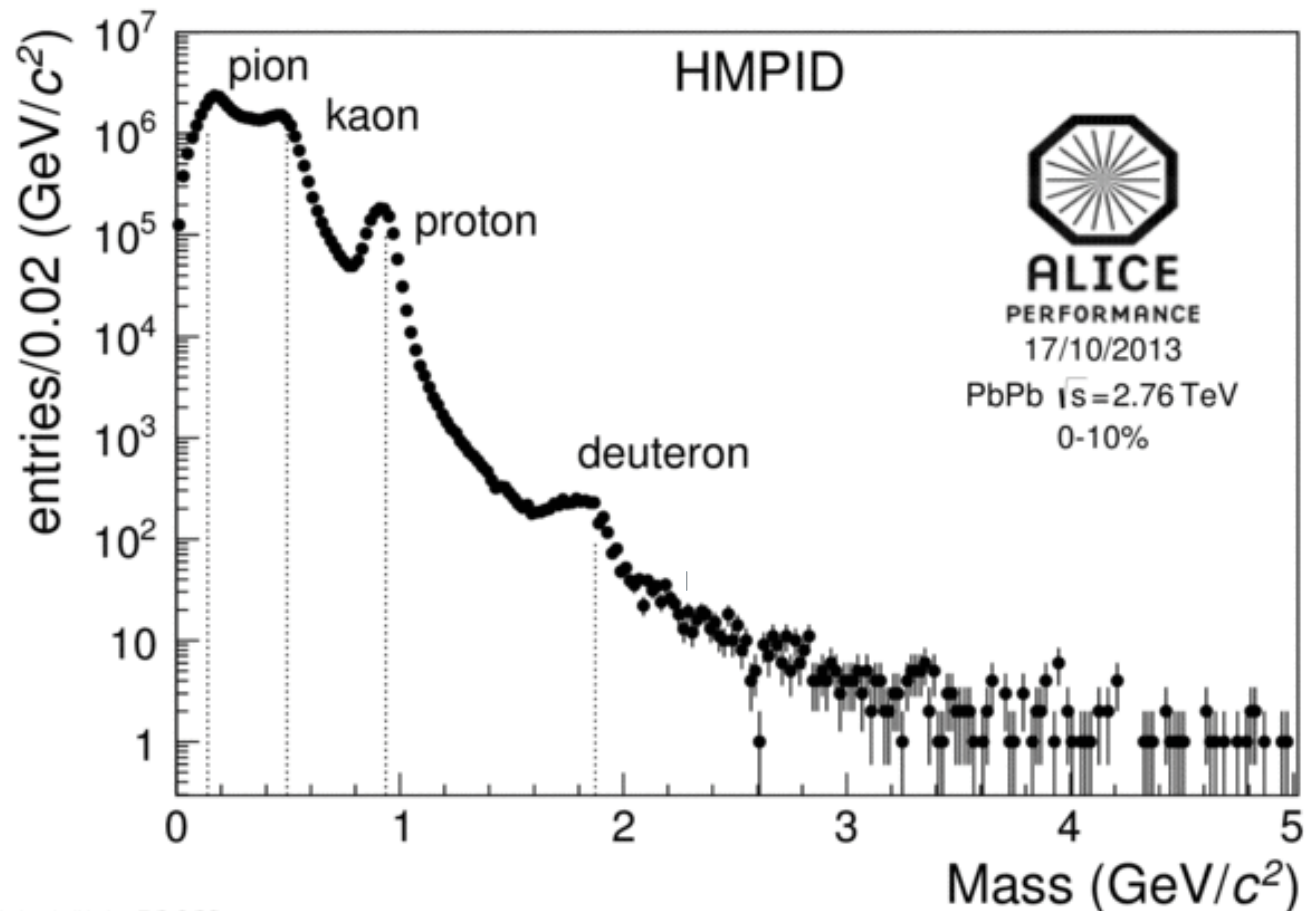- Particle identification via velocity measurement

High Momentum PID (HMPID):
- particle identification via ring imaging Cherenkov

A Large Ion Collider Experiment

ALICE particle identification capabilities are unique. Almost all known techniques are exploited: dE/dx, Time Of Flight, Transition Radiation, Cherenkov Radiation, calorimetry and decay topology (V0, cascade).

Inner Tracking System (ITS) :
- Primary vertex
- Tracking
- Particle identification via dE/dx

Time Projection Chamber (TPC):
- Global tracking
- Particle identification via dE/dx

Time Of Flight (TOF):
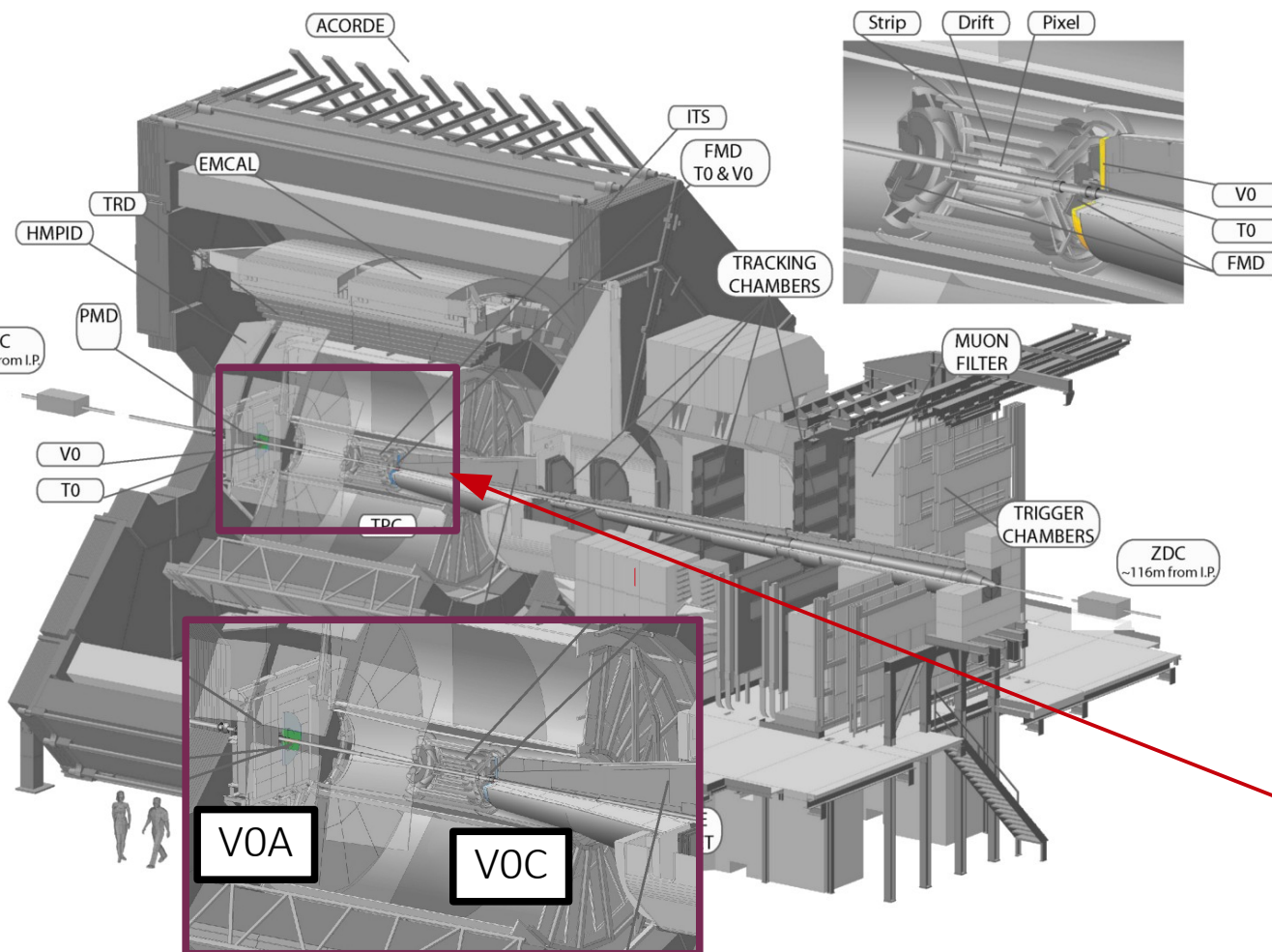- Particle identification via velocity measurement

High Momentum PID (HMPID):
- particle identification via ring imaging Cherenkov

A Large Ion Collider Experiment

ALICE particle identification capabilities are unique. Almost all known techniques are exploited: dE/dx, Time Of Flight, Transition Radiation, Cherenkov Radiation, calorimetry and decay topology (V0, cascade).

Inner Tracking System (ITS) :
- Primary vertex
- Tracking
- Particle identification via dE/dx

Time Projection Chamber (TPC):
- Global tracking
- Particle identification via dE/dx

Time Of Flight (TOF):
- Particle identification via velocity measurement

High Momentum PID (HMPID):
- particle identification via ring imaging Cherenkov

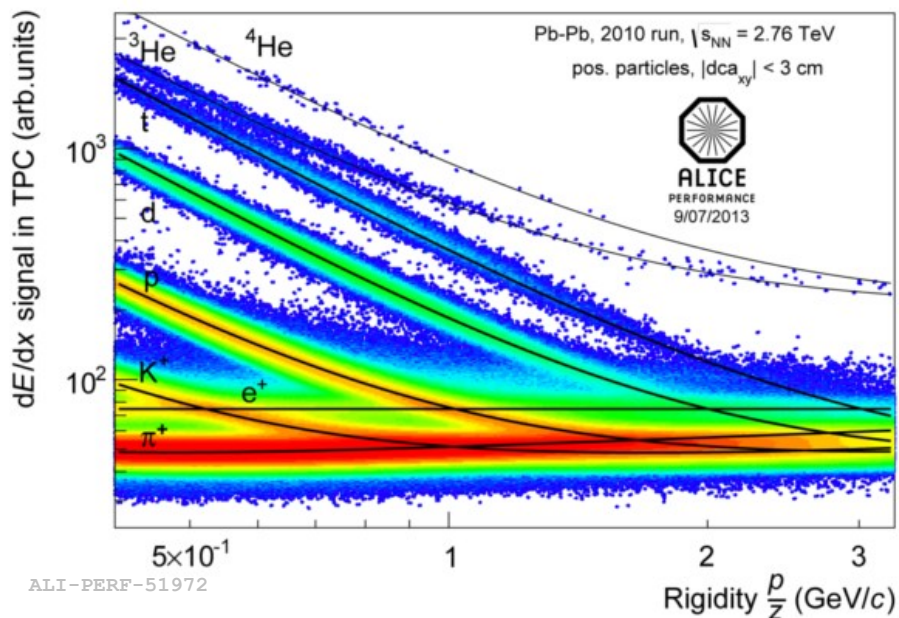**V0 (A-C)**: Trigger, beam-gas event rejection, multiplicity classes

Nuclei:
Identification and Results

Nuclei Identification

Low momenta

Nuclei identification via dE/dx measurement in the TPC:

- dE/dx resolution in central Pb-Pb collisions: 7%

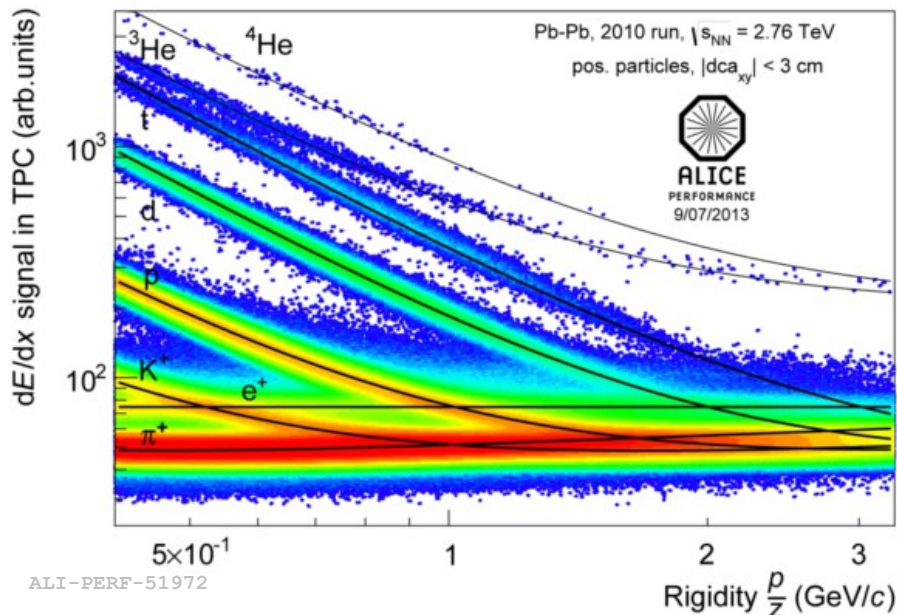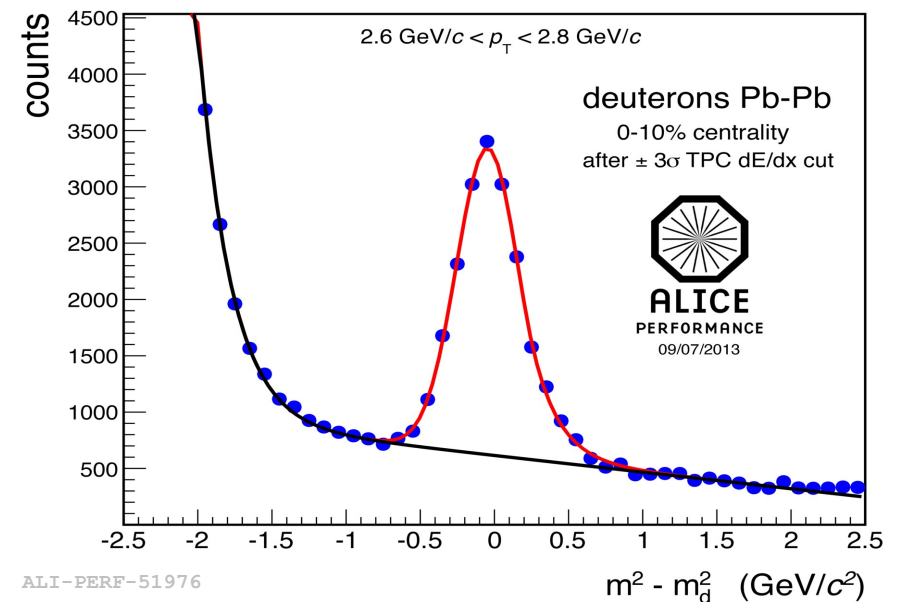- Excellent separation of (anti-)nuclei from other particles

ALI-PERF-51972

Nuclei Identification

Low momenta	Higher Momenta
Nuclei identification via dE/dx measurement in the TPC:	Velocity measurement with the Time Of Flight detector is used to evaluate the m^2 distribution.

Low momenta

Nuclei identification via dE/dx measurement in the TPC:

- dE/dx resolution in central Pb-Pb collisions: 7%

- Excellent separation of (anti-)nuclei from other particles

Higher Momenta

Velocity measurement with the Time Of Flight detector is used to evaluate the m^2 distribution.

- Excellent TOF performance: $\sigma_{TOF} \approx 85$ ps in Pb-Pb collisions.
- $\pm 3\sigma$-cut around expected TPC dE/dx for deuterons reduces drastically the background from TPC-TOF track mismatch
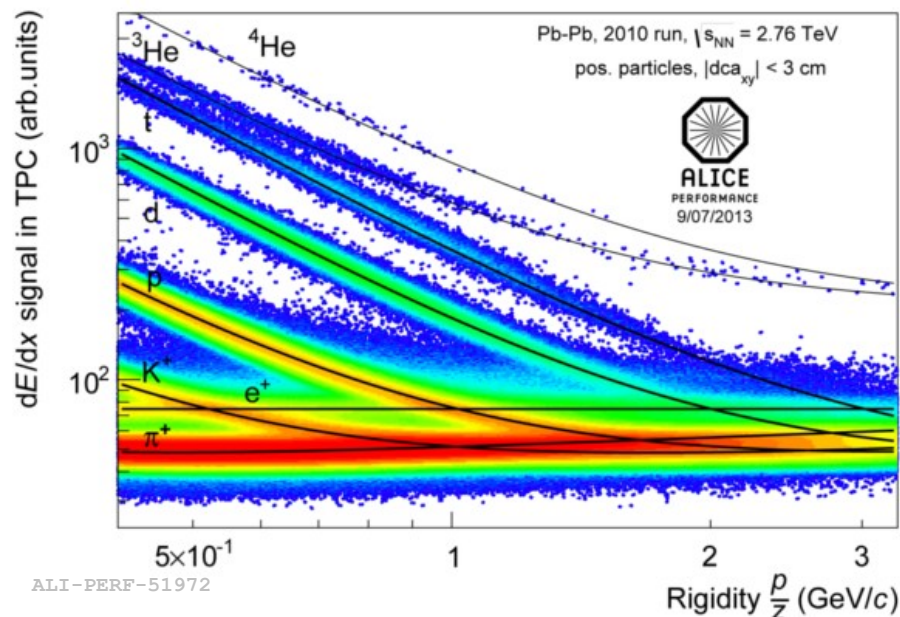
Nuclei Identification

Low momenta

Nuclei identification via dE/dx measurement in the TPC:

- dE/dx resolution in central Pb-Pb collisions: 7%

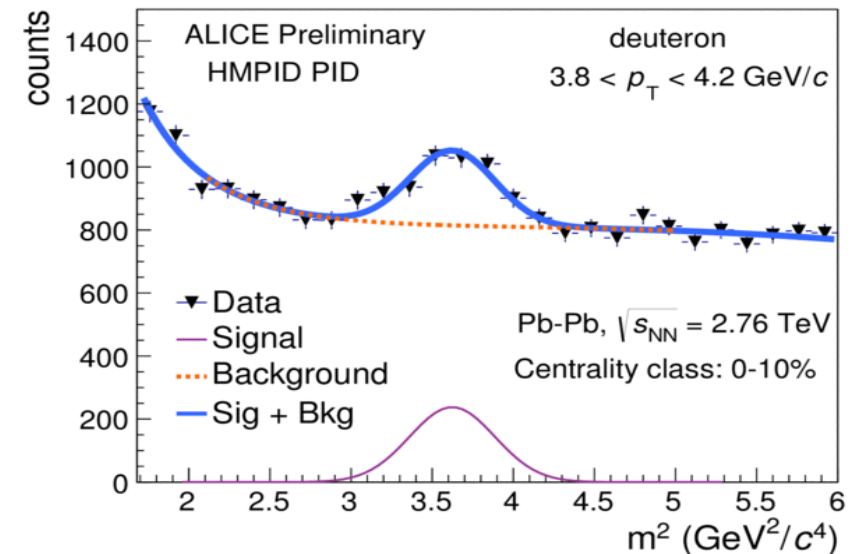- Excellent separation of (anti-)nuclei from other particles

Higher Momenta

HMPID

- At higher momenta nuclei in central Pb-Pb collisions are identified based on Cherenkov radiation with HMPID

$$\cos\theta_{Cherenkov} = \frac{1}{n\beta}$$

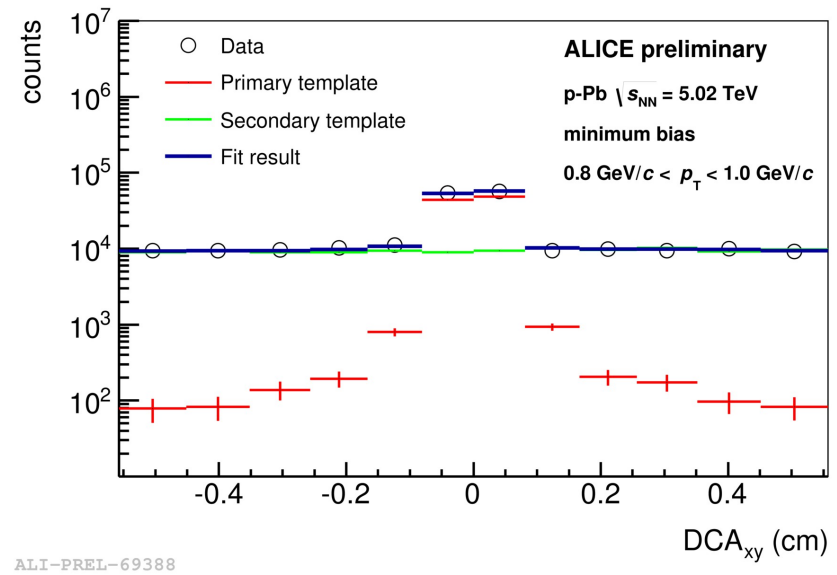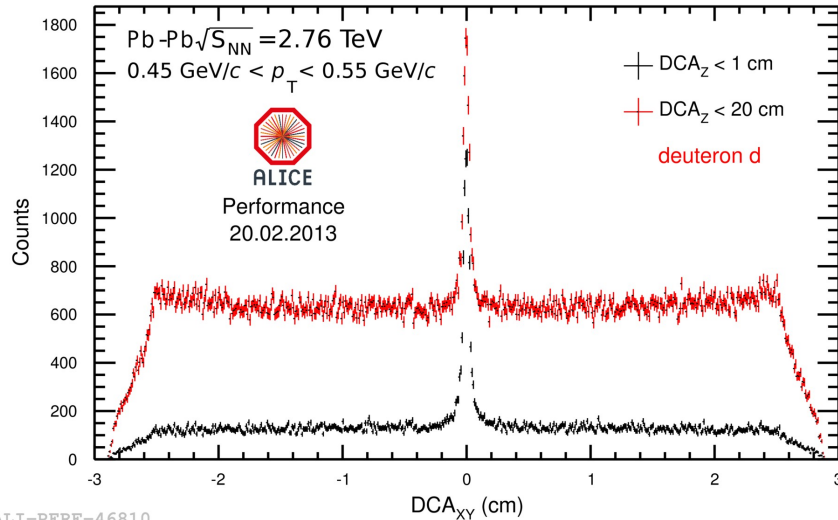$$m^2 = p^2\left(n^2\cos^2\theta_{Cherenkov} - 1\right)$$

Nuclei Identification : Secondaries

The measurement of nuclei is strongly affected by background from knock-out from material

→ Rejection is possible by applying a cut on DCA_Z and fitting the DCA_{XY} distributions with MC templates
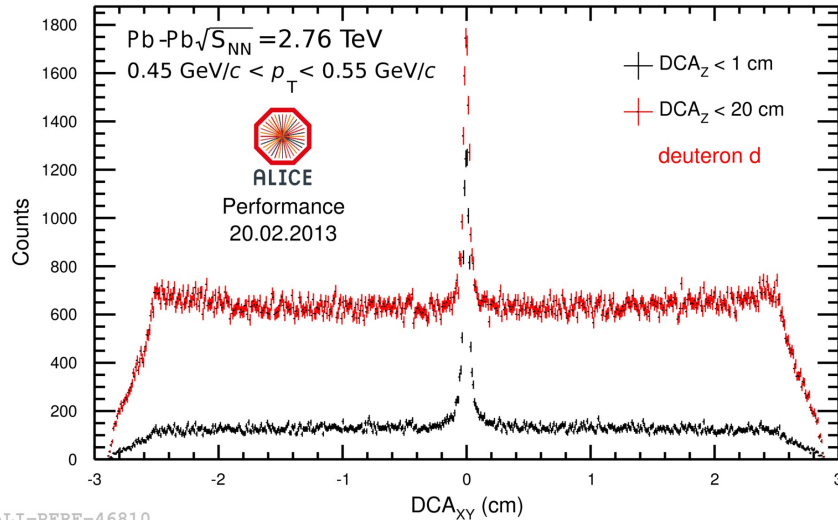
Nuclei Identification : Secondaries

The measurement of nuclei is strongly affected by background from knock-out from material

→ Rejection is possible by applying a cut on DCA_Z and fitting the DCA_{XY} distributions with MC templates

ALI−PERF−46810

ALI−PREL−69388
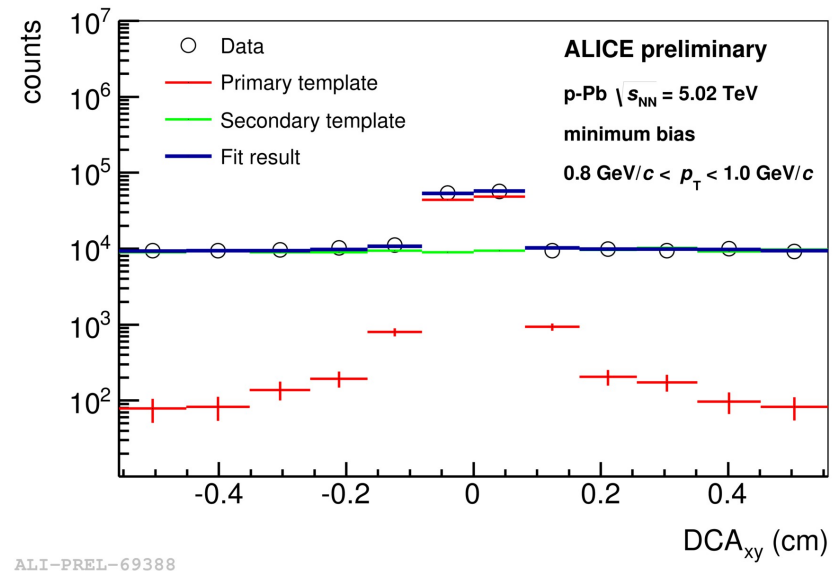
Not relevant for anti-nuclei. However, their measurement suffers from large systematics related to unknown hadronic interaction cross-sections of anti-nuclei in material

Geometry of the collision
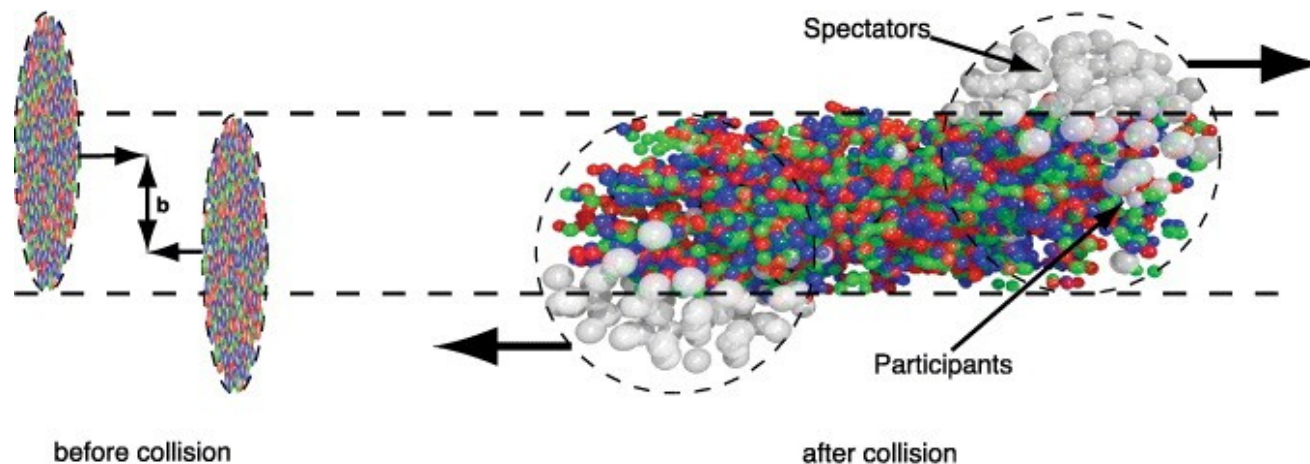
before collision

after collision

Spectators

Participants

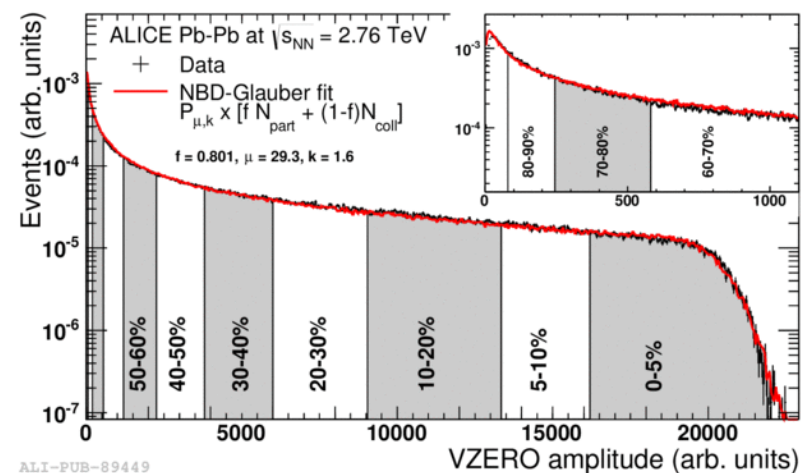Centrality = degree of overlap of the 2 colliding nuclei

Central collisions:
- small impact parameter b
- high number of participant nucleons $\rightarrow$ high multiplicity

Peripheral collisions:
- large impact parameter b
- low number of participant nucleons $\rightarrow$ low multiplicity

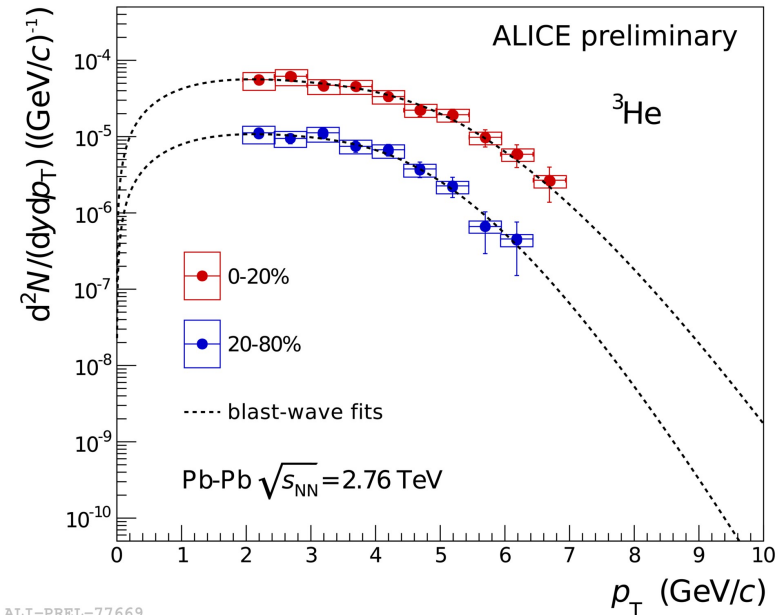Centrality connected to observables via Glauber model

ALICE Pb-Pb at $\sqrt{s_{NN}}$ = 2.76 TeV
+ Data
— NBD-Glauber fit
$P_{\mu,k} \times [f\, N_{part} + (1-f)N_{coll}]$
f = 0.801, μ = 29.3, k = 1.6

Events (arb. units)

VZERO amplitude (arb. units)

ALI-PUB-89449

K. Aamodt et al. (ALICE Collaboration) Phys. Rev. Lett. 106, 032301 (2011)

Deuterons and ^{3}He in Pb $-$ Pb
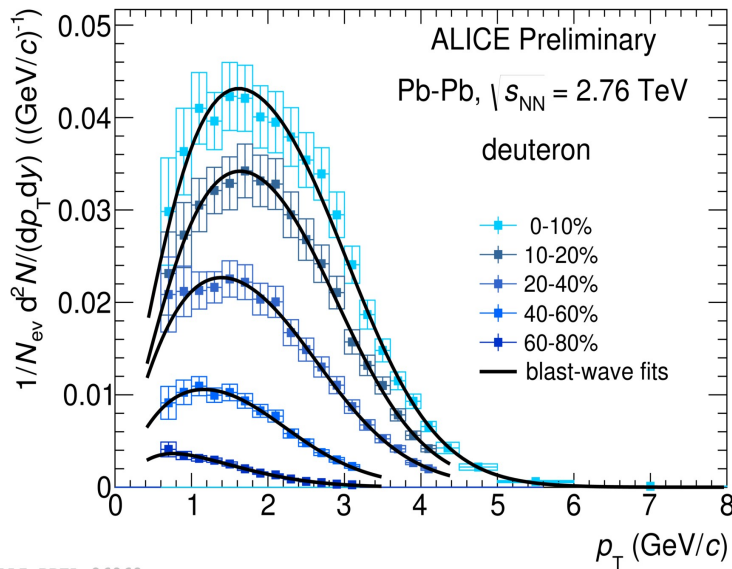

ALI-PREL-86969

ALI-PREL-77669

- Spectra are extracted in different centrality bins and fitted with a Blast-Wave function (simplified hydro model) for the extraction of yields (extrapolation to unmeasured region at low and high p_T)

  - ➢ A hardening of the spectrum with increasing centrality is observed as expected in a hydrodynamic description of the fireball as a radially expanding source

Blast-Wave model: E. Schnedermann et al., Phys. Rev. C 48, 2462 (1993)
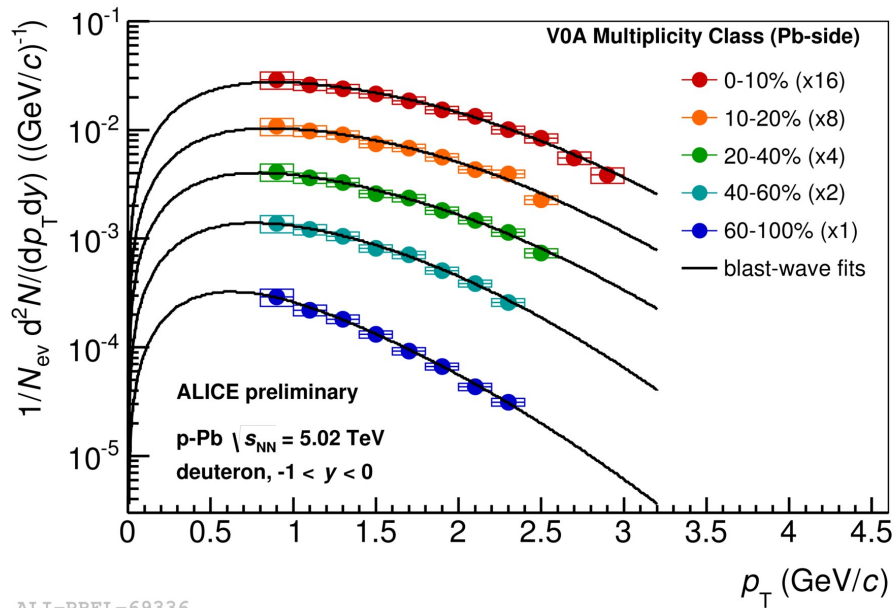
(Anti-)deuterons in p − Pb
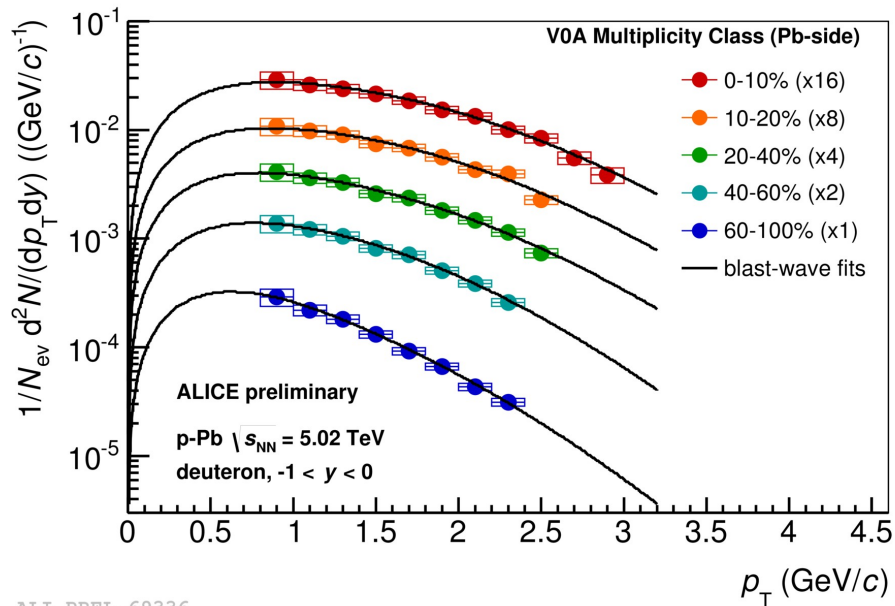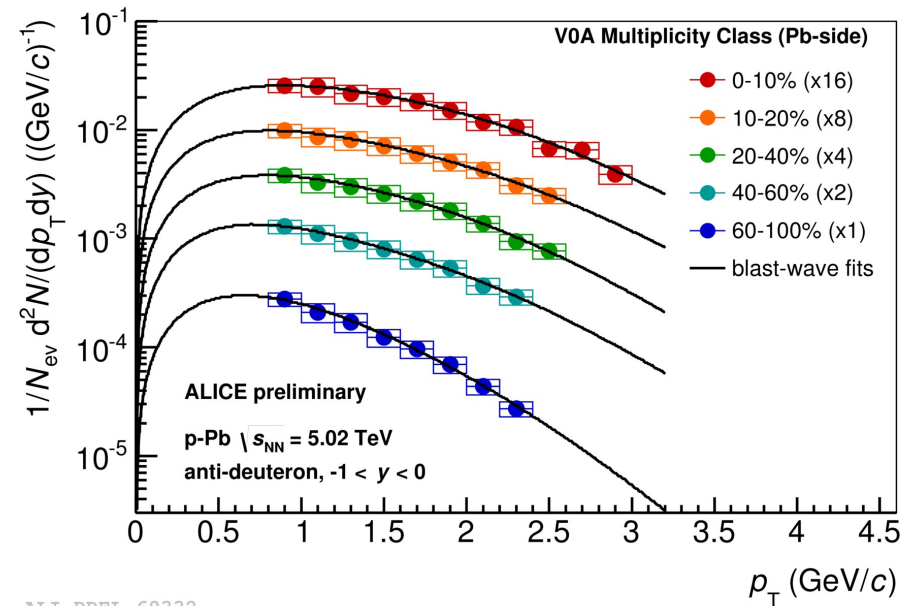
ALI−PREL−69336

ALI−PREL−69332

- Deuteron and anti-deuteron spectra extracted in different multiplicity bins and fitted with Blast-Wave functions for the extraction of yields
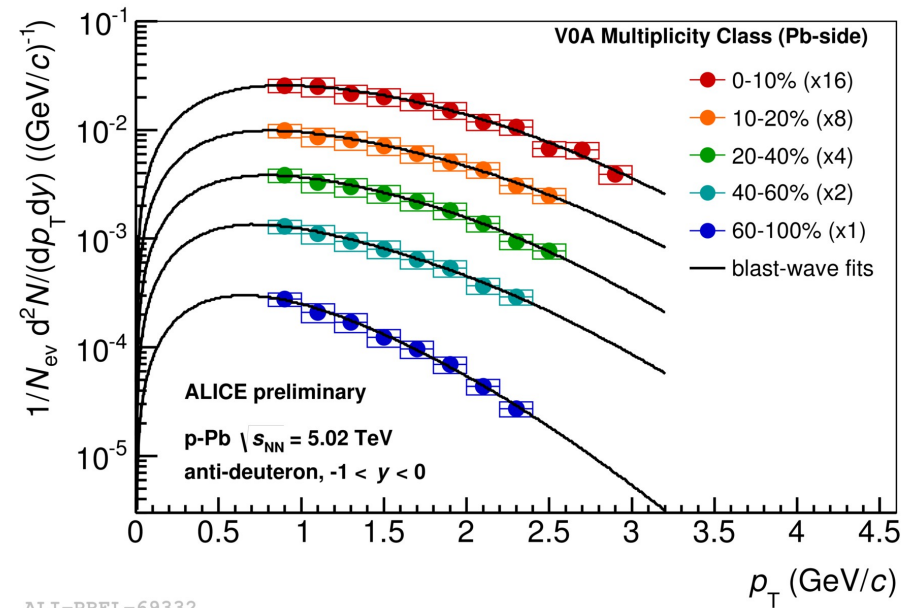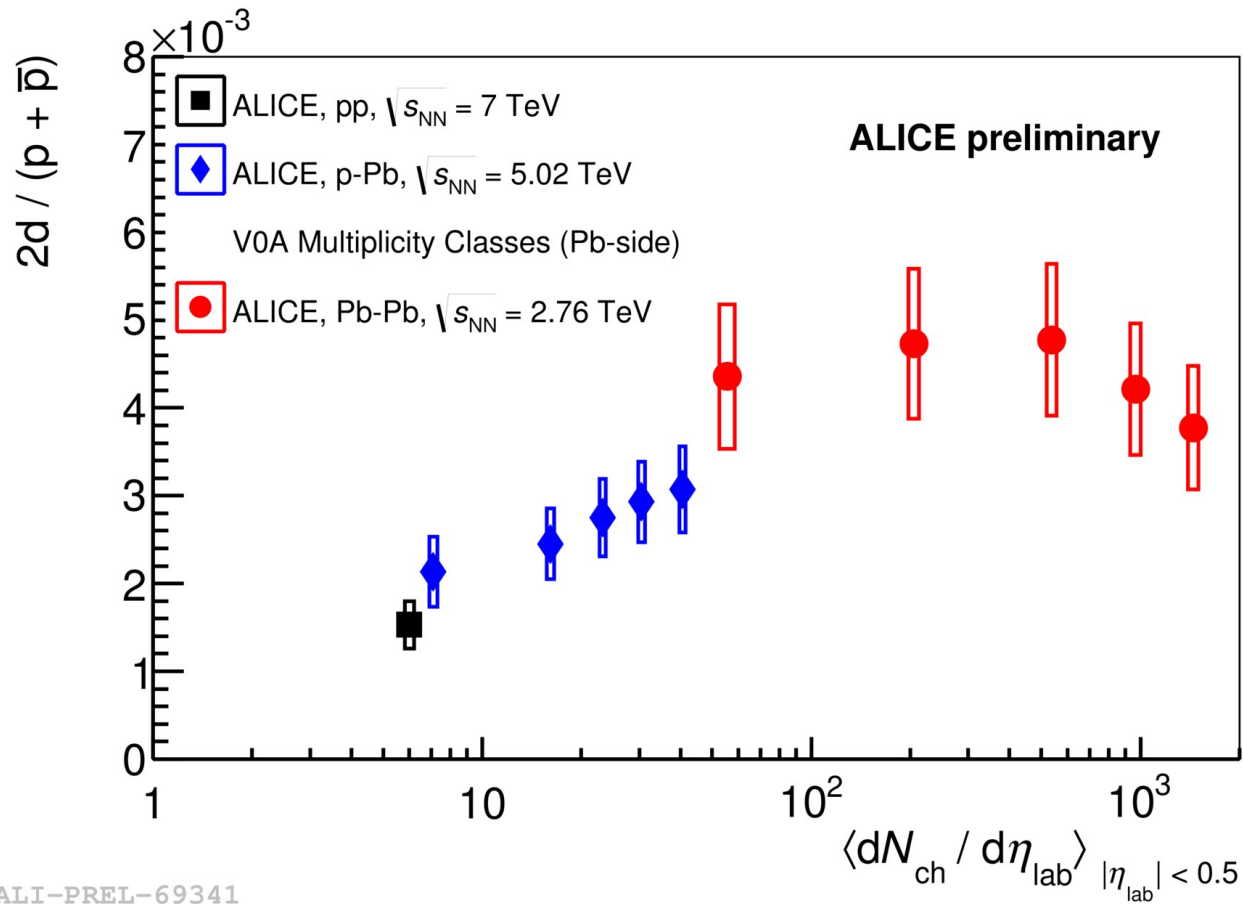
(Anti-)deuterons in p − Pb
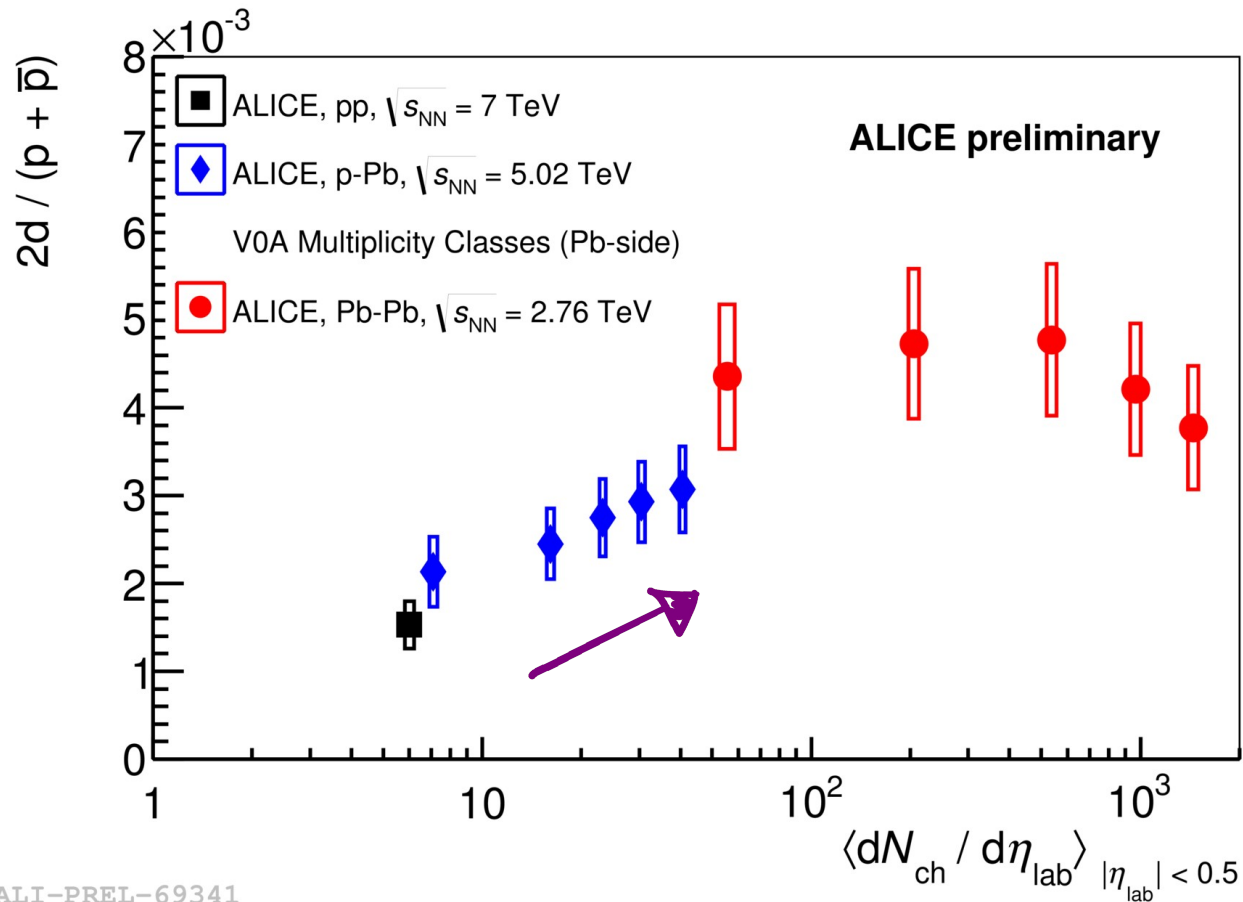

ALI−PREL−69336

ALI−PREL−69332

- Deuteron and anti-deuteron spectra extracted in different multiplicity bins and fitted with Blast-Wave functions for the extraction of yields
- Also in p-Pb collisions spectra become harder with increasing multiplicity

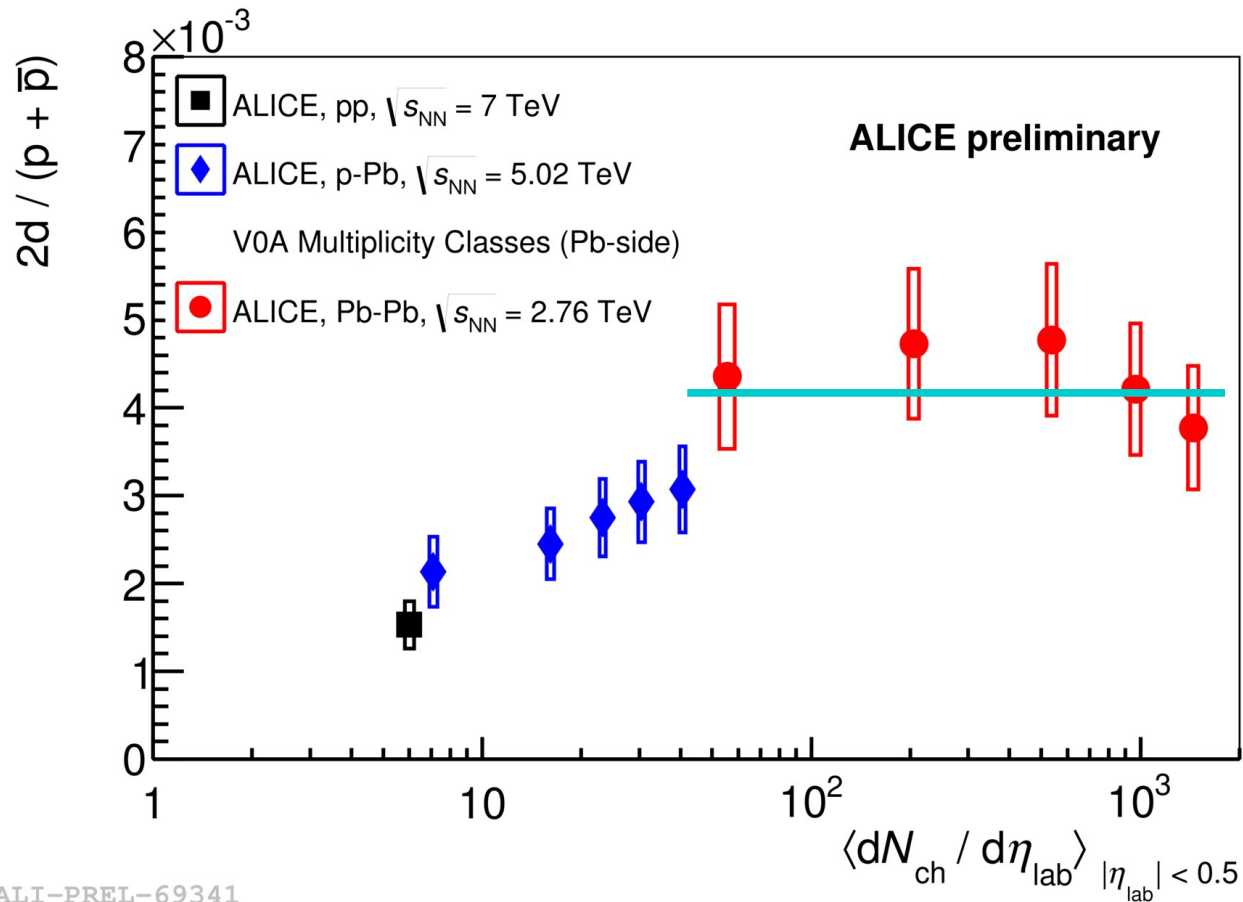# Deuteron to proton ratio

Deuteron to proton ratio

- Rise with multiplicity in p-Pb

ALI-PREL-69341

Deuteron to proton ratio

- Rise with multiplicity in p-Pb

- No significant centrality dependence in Pb-Pb

Figure legend:
- ALICE, pp, $\sqrt{s_{NN}}$ = 7 TeV
- ALICE, p-Pb, $\sqrt{s_{NN}}$ = 5.02 TeV
- V0A Multiplicity Classes (Pb-side)
- ALICE, Pb-Pb, $\sqrt{s_{NN}}$ = 2.76 TeV

ALICE preliminary

Y-axis: $2d / (p + \bar{p})$, $\times 10^{-3}$
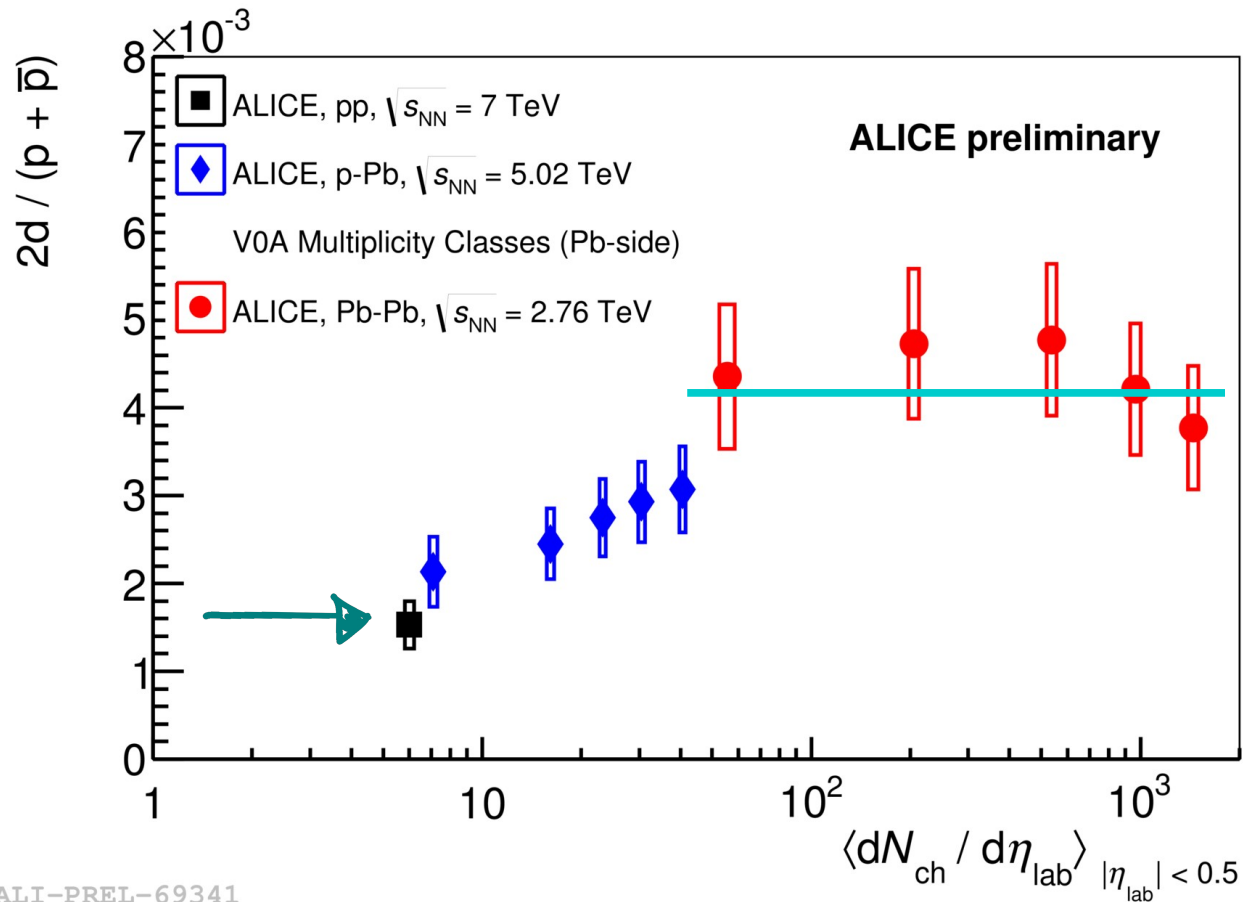
X-axis: $\langle dN_{ch} / d\eta_{lab} \rangle_{|\eta_{lab}| < 0.5}$

ALI–PREL–69341

Deuteron to proton ratio

- Rise with multiplicity in p-Pb

- No significant centrality dependence in Pb-Pb

- Ratio in pp collisions is a factor 2.5 lower than in Pb-Pb collisions

ALI−PREL−69341

$^3_\Lambda$H Identification and Results

$^3_{\Lambda}H$ is the lightest known hypernucleus and is formed by (p,n,Λ).

Mass = 2.991 GeV/c^2 B_{Λ} = 0.13 ± 0.05 MeV   Lifetime ~ 263 ps

Decay Channels	
$^3_{\Lambda}H \rightarrow\ ^3He + \pi^-$	$^3_{\bar{\Lambda}}\overline{H} \rightarrow\ ^3\overline{He} + \pi^+$
$^3_{\Lambda}H \rightarrow H + \pi^0$	$^3_{\bar{\Lambda}}\overline{H} \rightarrow \overline{H} + \pi^0$
$^3_{\Lambda}H \rightarrow d + p + \pi^-$	$^3_{\bar{\Lambda}}\overline{H} \rightarrow \overline{d} + \overline{p} + \pi^+$
$^3_{\Lambda}H \rightarrow d + n + \pi^-$	$^3_{\bar{\Lambda}}\overline{H} \rightarrow \overline{d} + \overline{n} + \pi^+$

$^3_{\Lambda}H$ and $^3_{\bar{\Lambda}}\overline{H}$ search via two-body decays into charged particles:

- Two body decay: lower combinatorial background
- Charged particles: ALICE acceptance, detection efficiency and momentum measurement for charged particles higher than for neutrals

Signal Extraction:
- Identify ^3He and π
- Evaluate (^3He,π) invariant mass
- Apply topological cuts in order to:
  - identify secondary decay vertex
  - reduce combinatorial background
- Extract signal

$\left({}^{3}_{\overline{\Lambda}}\overline{H}\right)\ {}^{3}_{\Lambda}H$ Identification

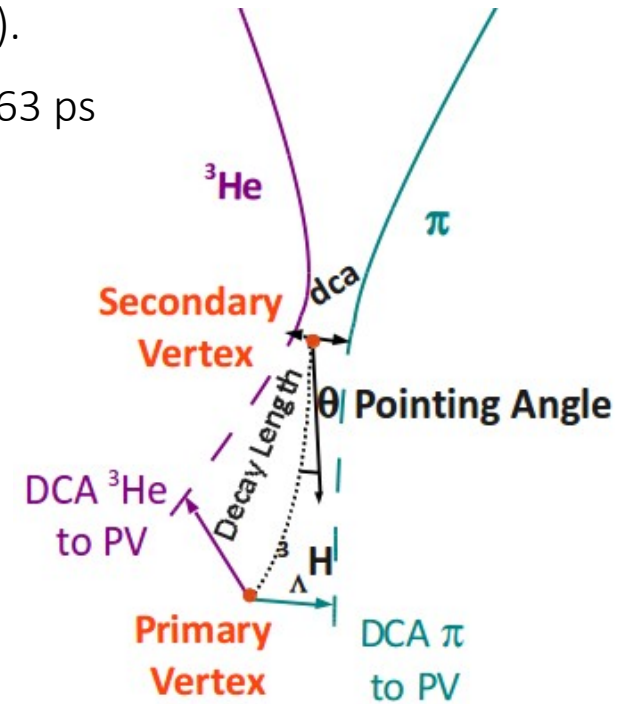${}^{3}_{\Lambda}H$ is the lightest known hypernucleus and is formed by (p,n,Λ).
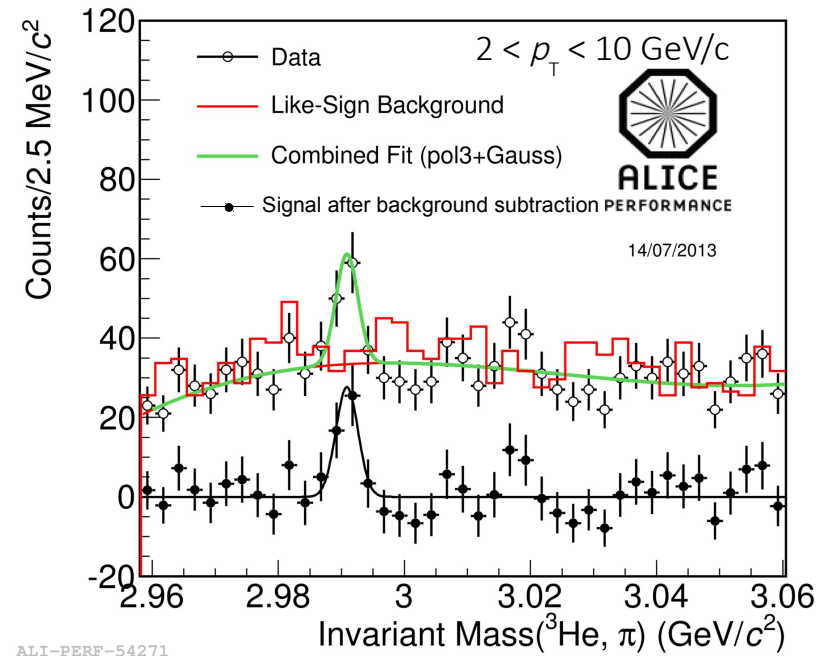
Mass = 2.991 GeV/c^2 B_{Λ} = 0.13 ± 0.05 MeV   Lifetime ~ 263 ps

Decay Channels	
${}^{3}_{\Lambda}H \rightarrow {}^{3}He + \pi^{-}$	${}^{3}_{\overline{\Lambda}}\overline{H} \rightarrow {}^{3}\overline{He} + \pi^{+}$
${}^{3}_{\Lambda}H \rightarrow H + \pi^{0}$	${}^{3}_{\overline{\Lambda}}\overline{H} \rightarrow \overline{H} + \pi^{0}$
${}^{3}_{\Lambda}H \rightarrow d + p + \pi^{-}$	${}^{3}_{\overline{\Lambda}}\overline{H} \rightarrow \overline{d} + \overline{p} + \pi^{+}$
${}^{3}_{\Lambda}H \rightarrow d + n + \pi^{-}$	${}^{3}_{\overline{\Lambda}}\overline{H} \rightarrow \overline{d} + \overline{n} + \pi^{+}$

${}^{3}_{\Lambda}H$ and ${}^{3}_{\overline{\Lambda}}\overline{H}$ search via two-body decays into charged particles:

- Two body decay: lower combinatorial background
- Charged particles: ALICE acceptance, detection efficiency and momentum measurement for charged particles higher than for neutrals

$\left({}^{3}He,\pi^{-}\right)+ \left({}^{3}\overline{He},\pi^{+}\right)$ Invariant Mass spectrum

ALI−PERF−54271

μ = 2.992 ± 0.002 GeV/c^2
σ = (2.08 ± 0.50)x10^{-3} GeV/c^2

$\left({}^{3}_{\Lambda}\overline{H}\right)\,{}^{3}_{\Lambda}H$ dN/dy
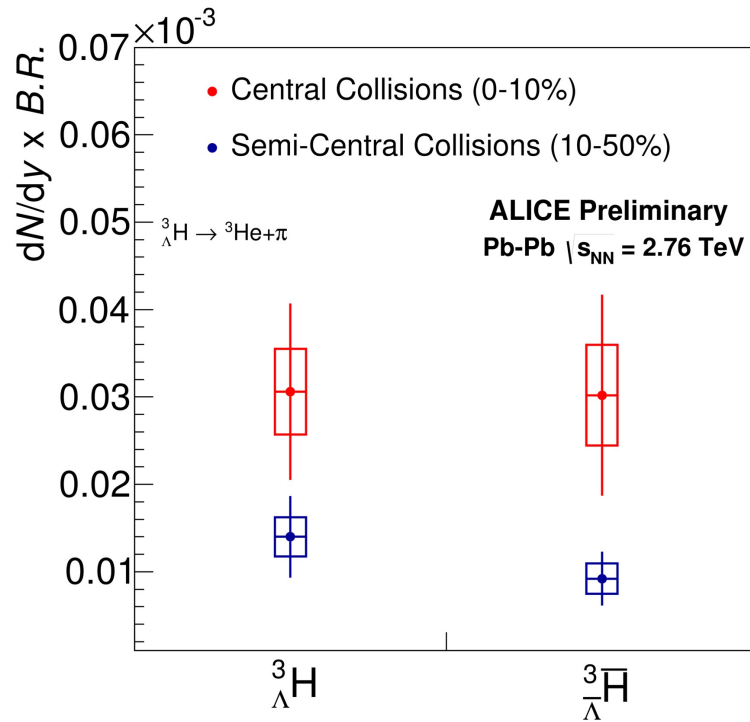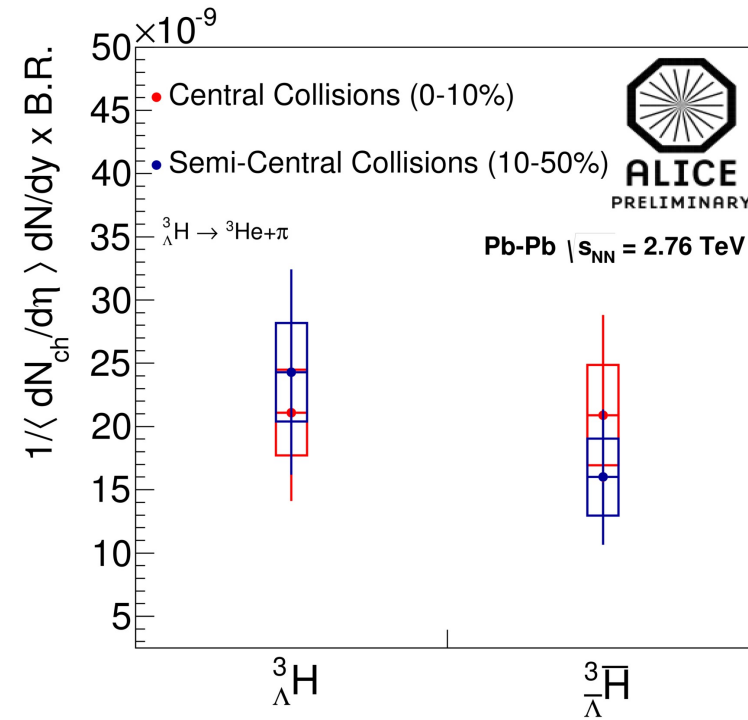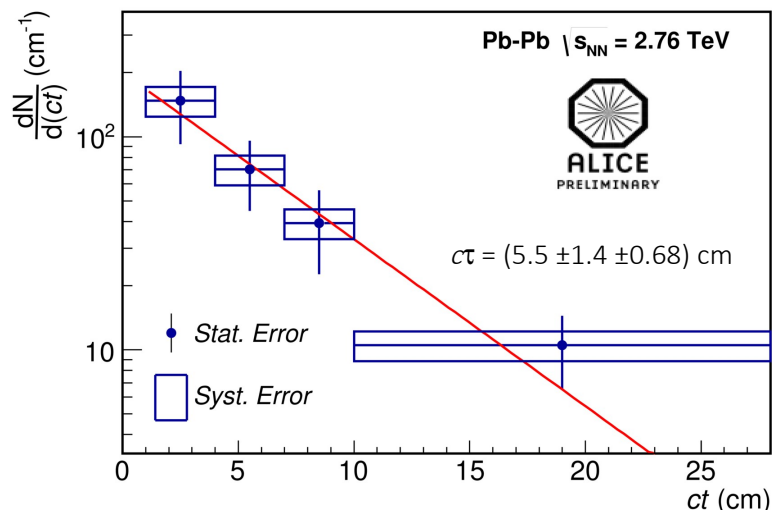

dN/dy x *B.R.* (${}^{3}_{\Lambda}H \rightarrow {}^{3}He + \pi^{-}$) extracted in two centrality bins for central (0-10%) and semi-central (10-50%) events and for ${}^{3}_{\Lambda}H$ and ${}^{3}_{\Lambda}\overline{H}$ separately

$\left(^3_{\overline{\Lambda}}\overline{H}\right)~^3_\Lambda H~dN/dy$
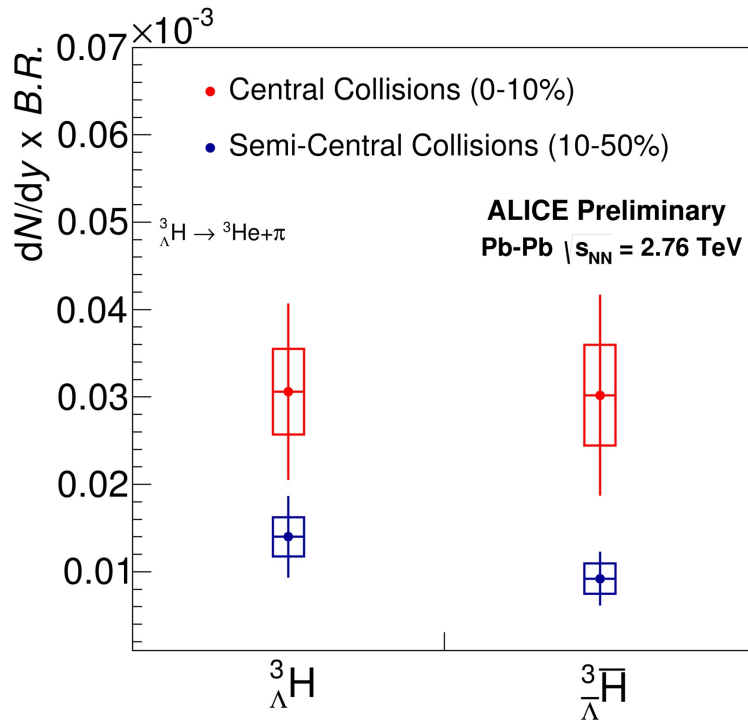
ALI-PREL-54275

dN/dy x *B.R.* ($^3_\Lambda$H → ^{3}He + π$^-$) extracted in two centrality bins for central (0-10%) and semi-central (10-50%) events and for $^3_\Lambda$H and $^3_{\overline{\Lambda}}\overline{H}$ separately

ALI-PREL-54279

Assuming particle production scales with centrality, yields were renormalized by <dN$_{ch}$/dη>:

✔ Central and semi-Central yields consistent after scaling

K. Aamodt et al. (ALICE Collaboration) Phys. Rev. Lett. 106, 032301 (2011)

$^3_\Lambda$H Lifetime determination

Pb-Pb $\sqrt{s_{NN}}$ = 2.76 TeV

ALICE PRELIMINARY

$c\tau$ = (5.5 ±1.4 ±0.68) cm

- Stat. Error
- Syst. Error

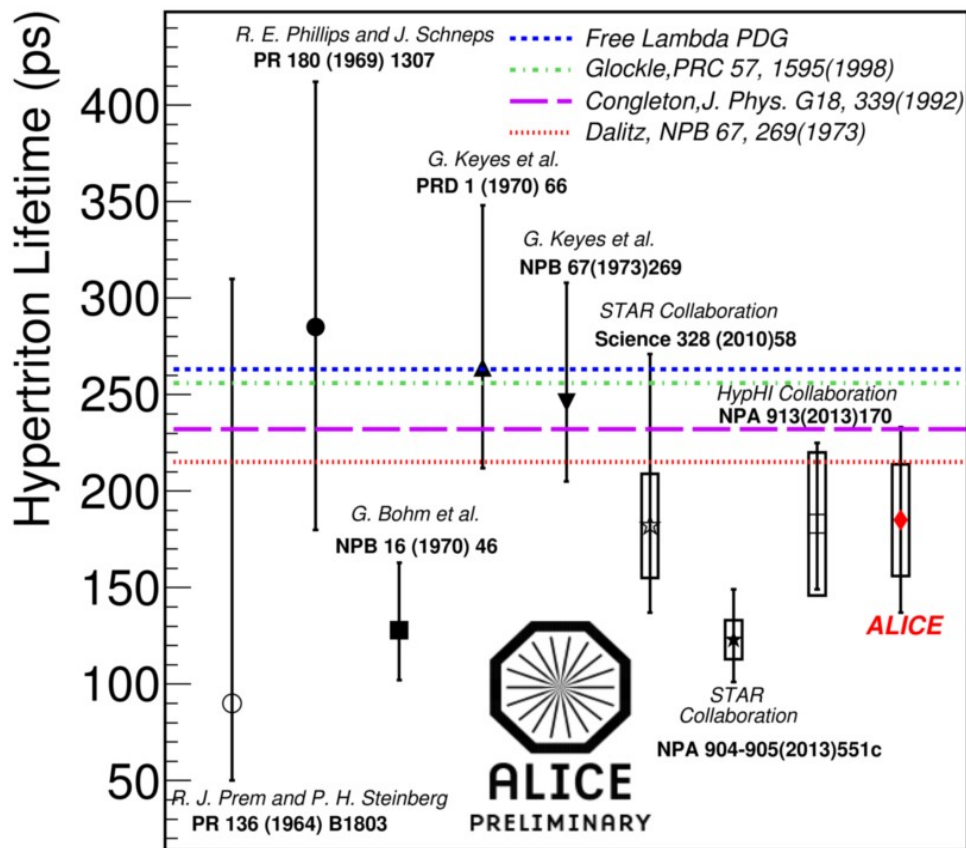ALI-PREL-54387

Direct decay time measurement is difficult (~ps), but the excellent determination of primary and decay vertex allows measurement of lifetime via:

$$N(t) = N(0)\exp\left(-\frac{L}{\beta\gamma c\tau}\right)$$

Where $c\tau = mL/p$ (cm)
With m the hypertriton mass, L the decay length and p the total momentum

R. E. Phillips and J. Schneps
PR 180 (1969) 1307
····· Free Lambda PDG
─·─· Glockle, PRC 57, 1595(1998)
── Congleton, J. Phys. G18, 339(1992)
····· Dalitz, NPB 67, 269(1973)

G. Keyes et al.
PRD 1 (1970) 66

G. Keyes et al.
NPB 67(1973)269

STAR Collaboration
Science 328 (2010)58

HypHI Collaboration
NPA 913(2013)170

G. Bohm et al.
NPB 16 (1970) 46

ALICE

STAR Collaboration
NPA 904-905(2013)551c

ALICE PRELIMINARY

R. J. Prem and P. H. Steinberg
PR 136 (1964) B1803

ALI-PREL-54325

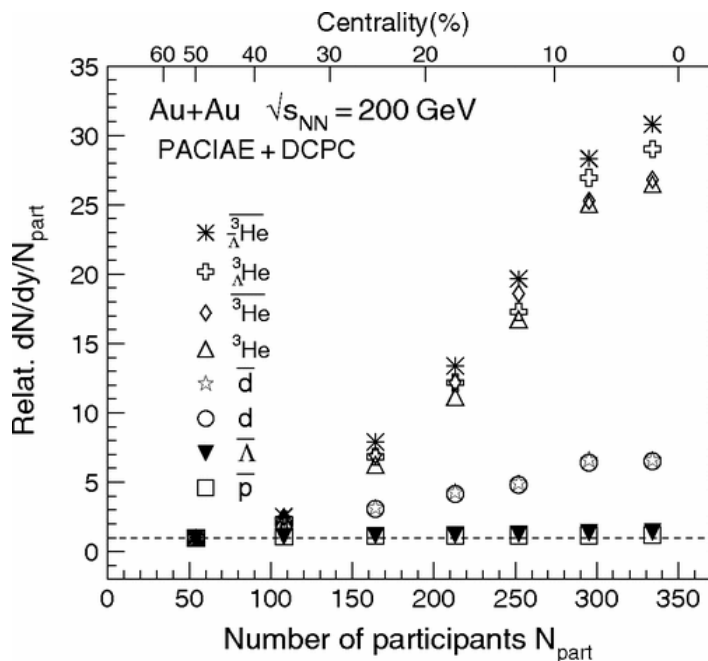$c\tau$ = (5.5 ±1.4 ±0.68) cm

τ = 185 ± 48 ± 29 ps

Model Comparison:
Coalescence vs. Thermal Model

(Anti-)(Hyper)nuclei production

Coalescence

- If baryons at freeze-out are close enough in phase space an (anti-)(hyper)nucleus can be formed

- (Hyper)nuclei are formed by protons and neutrons (Λ) which have similar velocities after the kinetic freeze-out

G. Chen et al., Phys. Rev. C 88, 034908 (2013)

Within a coalescence approach, the formation probability of a nucleus can be quantified through the parameter B_A

$$B_A = \frac{E_A \dfrac{d^3 N_A}{dp_d^3}}{\left(E_p \dfrac{d^3 N_p}{dp_p^3} \right)^A}$$

$$B_2 = \frac{E_d \dfrac{d^3 N_d}{dp_d^3}}{\left(E_p \dfrac{d^3 N_p}{dp_p^3} \right)^2}$$

(deuterons)

In first order, B_2 is expected to depend only on the maximum difference in the momentum of the two constituents ("pure nuclear physics")

- B_2 should be flat vs. p_T and should not depend on multiplicity/centrality
- The d/p ratio should increase linearly with multiplicity/centrality (assuming p and n spectra are equal)
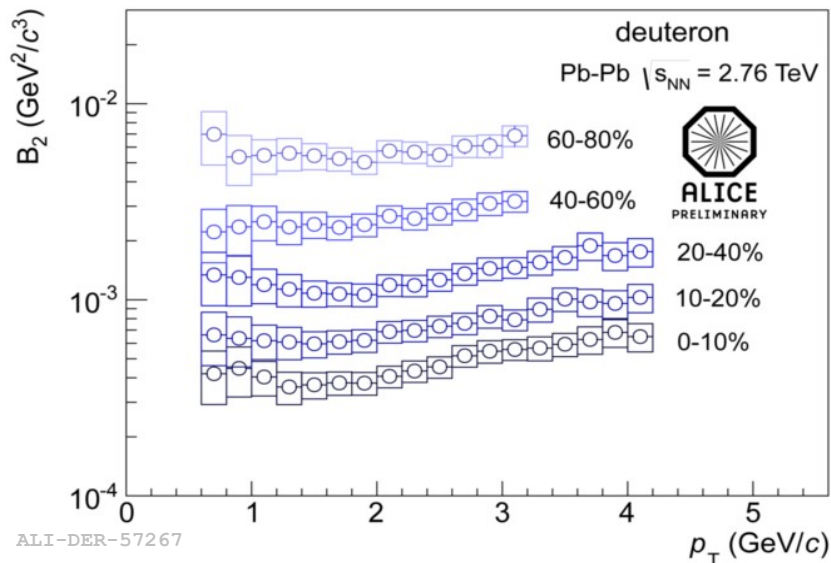
Deuterons B$_2$
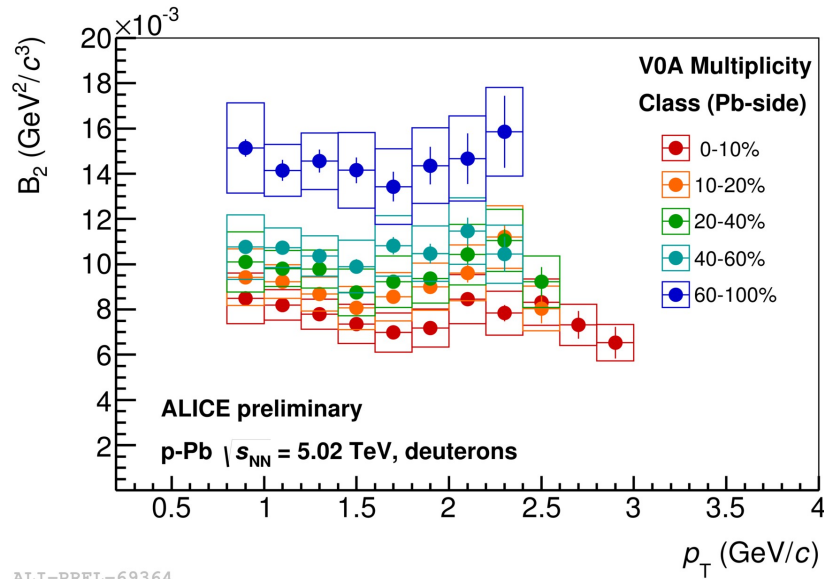
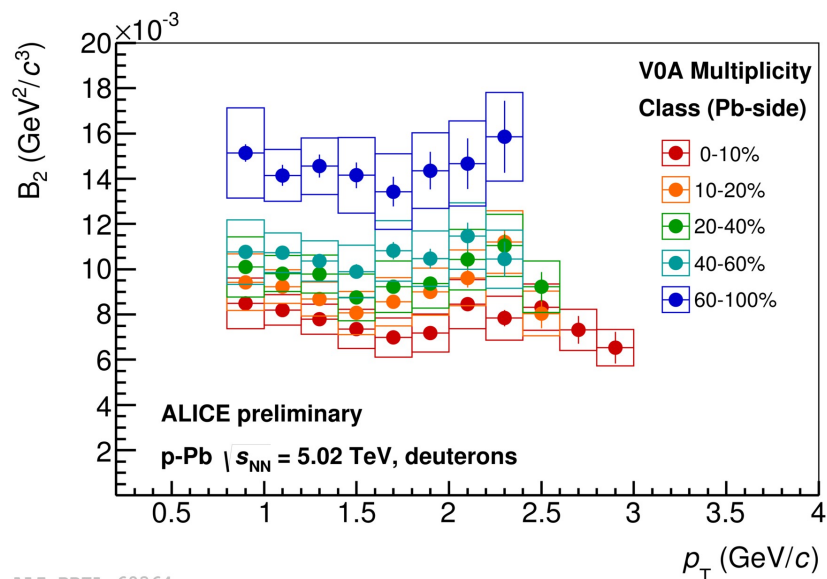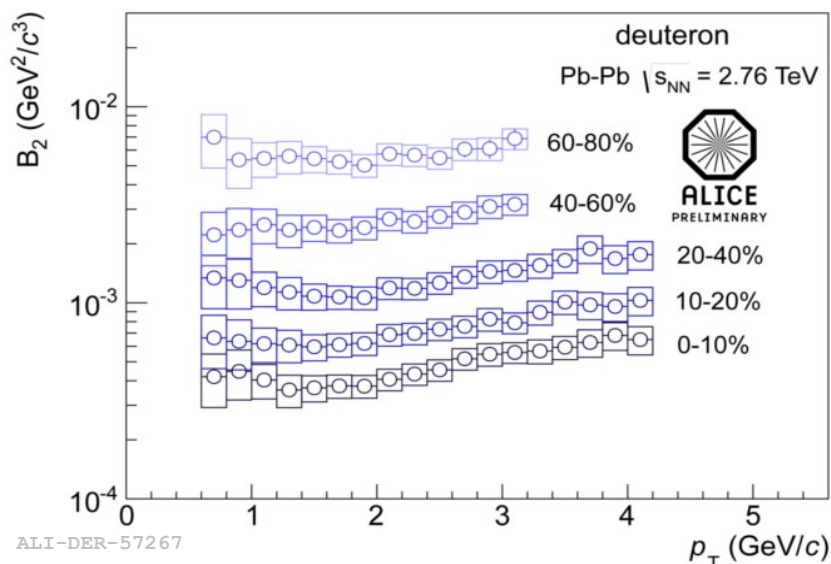ALI-PREL-69364

ALI-DER-57267

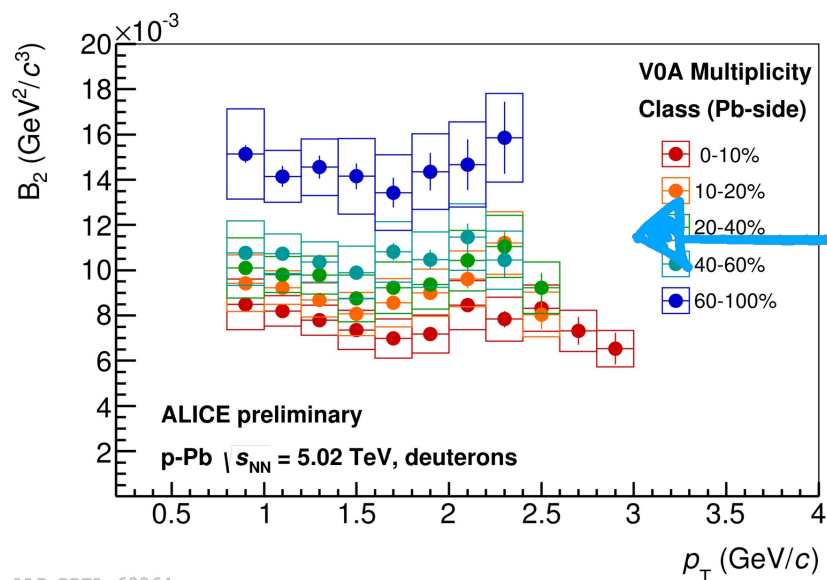Within a coalescence approach, the formation probability of deuterons can be quantified through the parameter B$_2$

$$B_2 = \frac{E_d \dfrac{d^3 N_d}{dp_d^3}}{\left(E_p \dfrac{d^3 N_p}{dp_p^3} \right)^2}$$
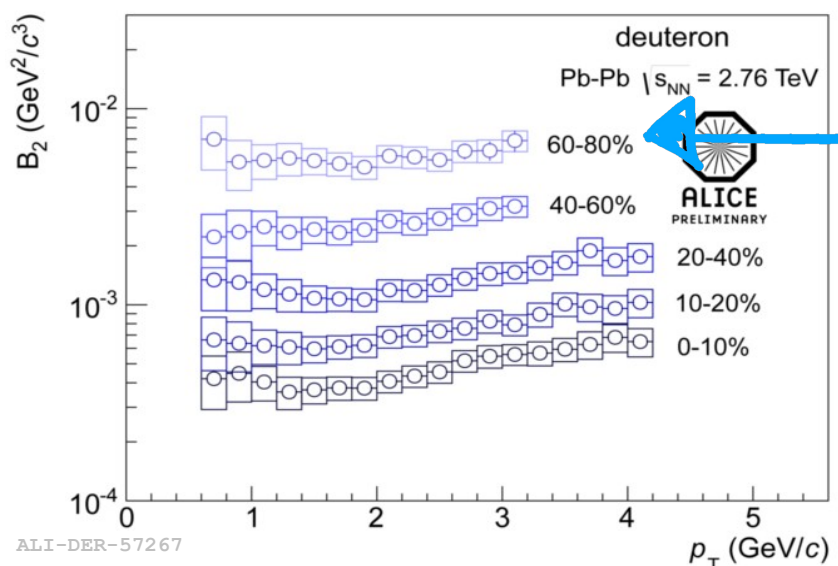
Deacons B$_2$

ALI-PREL-69364

ALI-DER-57267

Within a coalescence approach, the formation probability of deuterons can be quantified through the parameter B$_2$

$$B_2 = \frac{E_d \dfrac{d^3 N_d}{dp_d^3}}{\left(E_p \dfrac{d^3 N_p}{dp_p^3} \right)^2}$$

Simple coalescence model:
- Flat B$_2$ vs p_T and no dependence on multiplicity/centrality

Deuterons B$_2$

ALI-PREL-69364

ALI-DER-57267

Within a coalescence approach, the formation probability of deuterons can be quantified through the parameter B$_2$

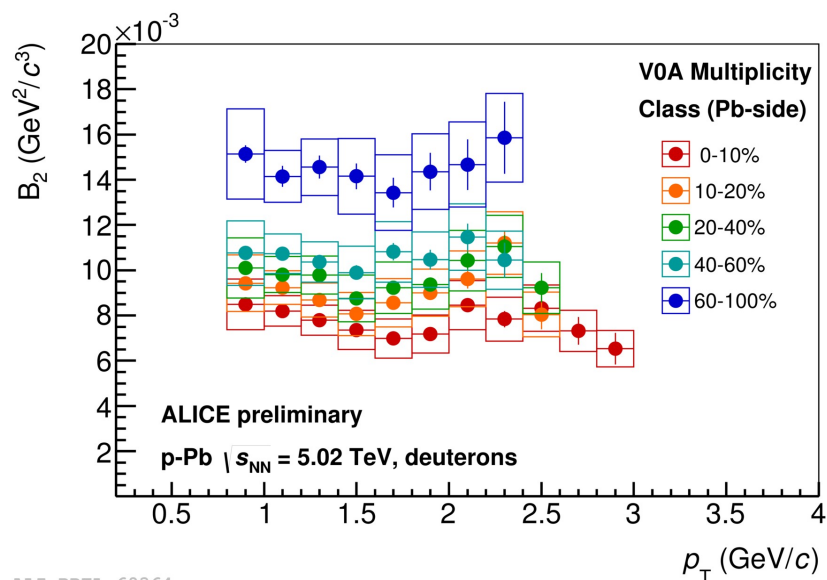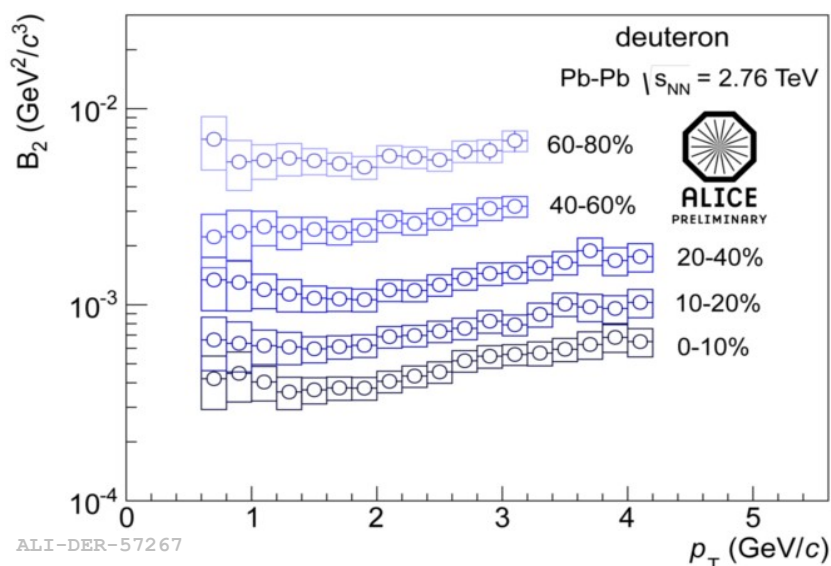$$B_2 = \frac{E_d \dfrac{d^3 N_d}{dp_d^3}}{\left(E_p \dfrac{d^3 N_p}{dp_p^3}\right)^2}$$

Simple coalescence model:
- Flat B$_2$ vs p_T and no dependence on multiplicity/centrality
  - ✔ Observed in p-Pb and peripheral Pb-Pb

Deuterons B$_2$

ALI-PREL-69364

ALI-DER-57267

Within a coalescence approach, the formation probability of deuterons can be quantified through the parameter B$_2$

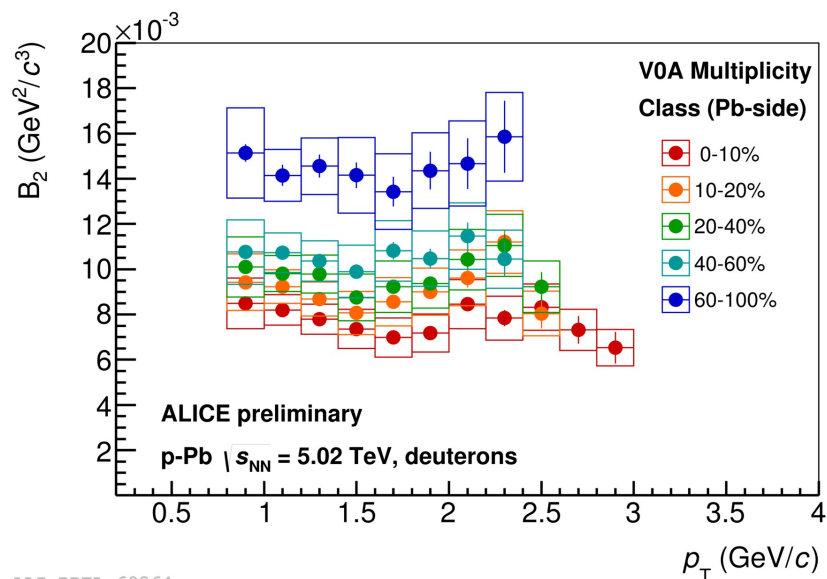$$B_2 = \frac{E_d \dfrac{d^3 N_d}{dp_d^3}}{\left(E_p \dfrac{d^3 N_p}{dp_p^3} \right)^2}$$

Simple coalescence model:
- Flat B$_2$ vs p_T and no dependence on multiplicity/centrality
    - ✔ Observed in p-Pb and peripheral Pb-Pb

More elaborated coalescence model:
- B$_2$ scales like HBT radii
    - ➢ decrease with centrality in Pb-Pb is explained as an increase in the source volume
    - ➢ increasing with p_T in central Pb-Pb reflects the k$_T$-dependence of the homogeneity volume in HBT

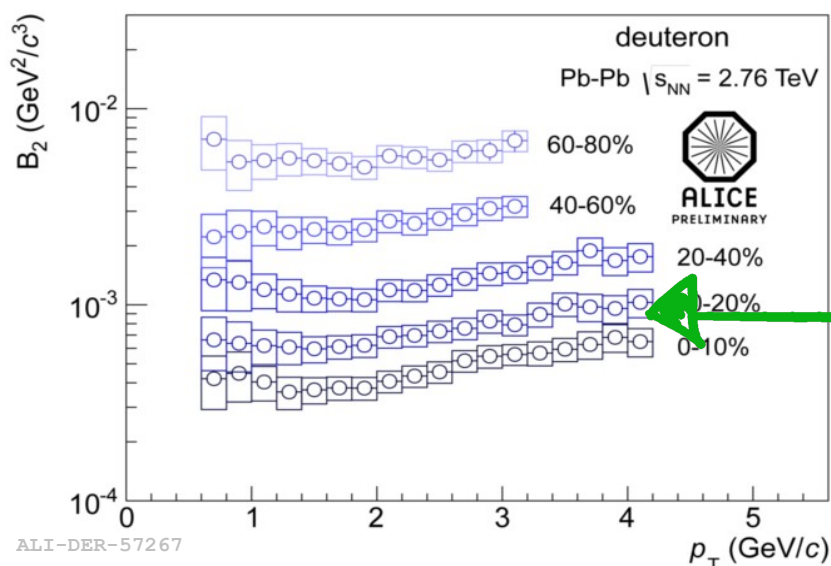# Deuterons B$_2$

ALI-PREL-69364

ALI-DER-57267

Within a coalescence approach, the formation probability of deuterons can be quantified through the parameter B$_2$

$$B_2 = \frac{E_d \dfrac{d^3 N_d}{dp_d^3}}{\left(E_p \dfrac{d^3 N_p}{dp_p^3} \right)^2}$$

Simple coalescence model:
- Flat B$_2$ vs p_T and no dependence on multiplicity/centrality
  - ✔ Observed in p-Pb and peripheral Pb-Pb

More elaborated coalescence model:
- B$_2$ scales like HBT radii
  - ➢ decrease with centrality in Pb-Pb is explained as an increase in the source volume
  - ➢ increasing with p_T in central Pb-Pb reflects the k_T-dependence of the homogeneity volume in HBT
    - ✔ Observed in central Pb-Pb collisions

(Anti-)(Hyper)nuclei production

Statistical thermal model

- Thermodynamic approach to particle production in heavy-ion collisions

- Abundances fixed at chemical freeze-out (T_{chem})

- For nuclei, it is a priori not clear that they can be described in a thermal picture:
  - The binding energy of the deuteron is E_B = 2.2 MeV and in principle, they should immediately dissociate in a medium with T_{ch} ≈ 160 MeV and be suppressed by a large factor

- However, it is the entropy per baryon which determines their production yield and this is fixed at chemical freeze-out [1]

- An observation of nuclei yields in agreement with thermal model is a sign for the adiabatic (isentropic expansion) in the hadronic phase
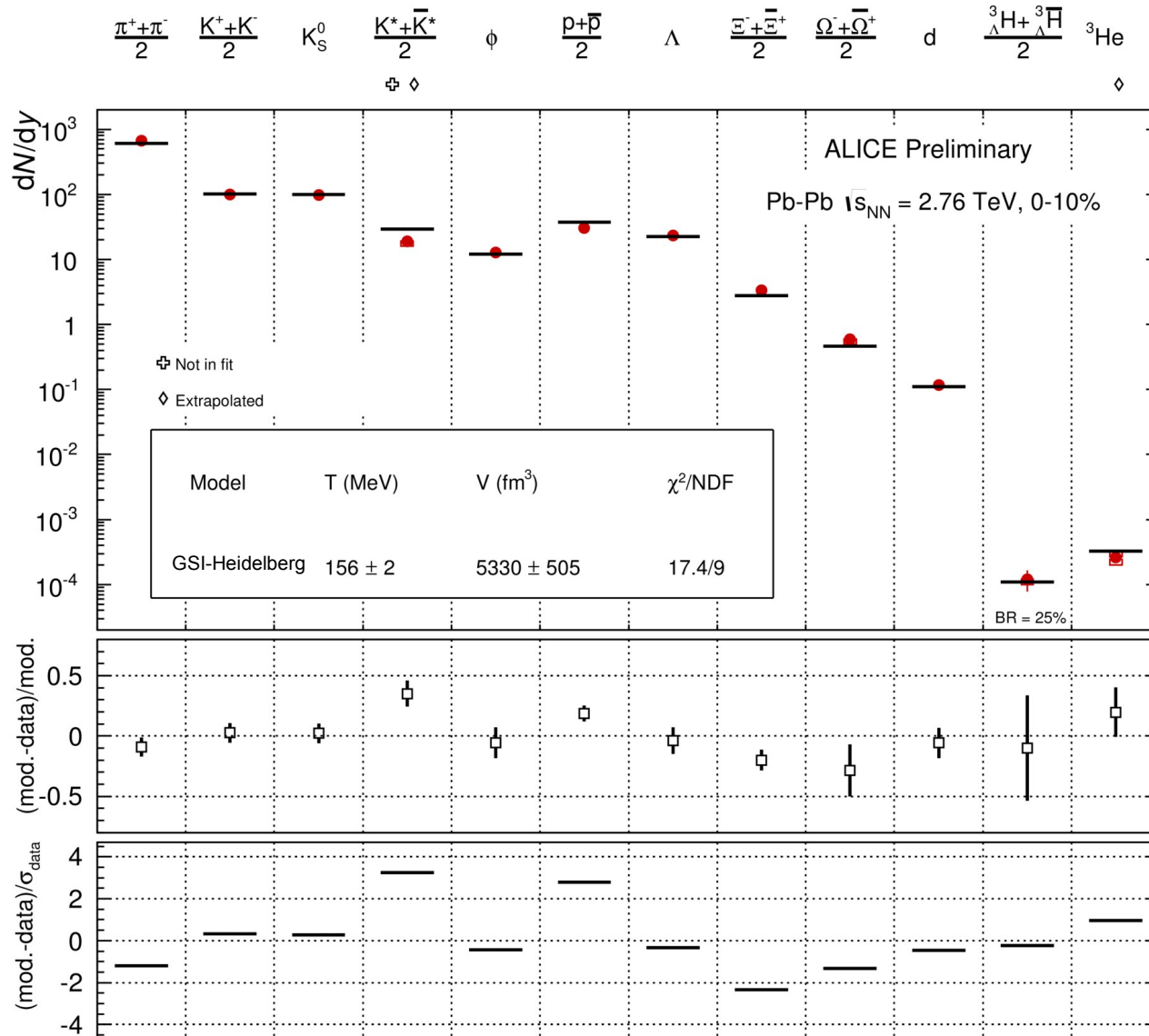
[1] P. Siemens and J. I. Kapusta, Phys.Rev.Lett. 43, 1486 (1979)

- (Hyper)nuclei are very sensitive to T_{chem} because of their large mass (M)
  - Exponential dependence of the yield: $dN/dy \propto e^{(-m/T_{chem})}$
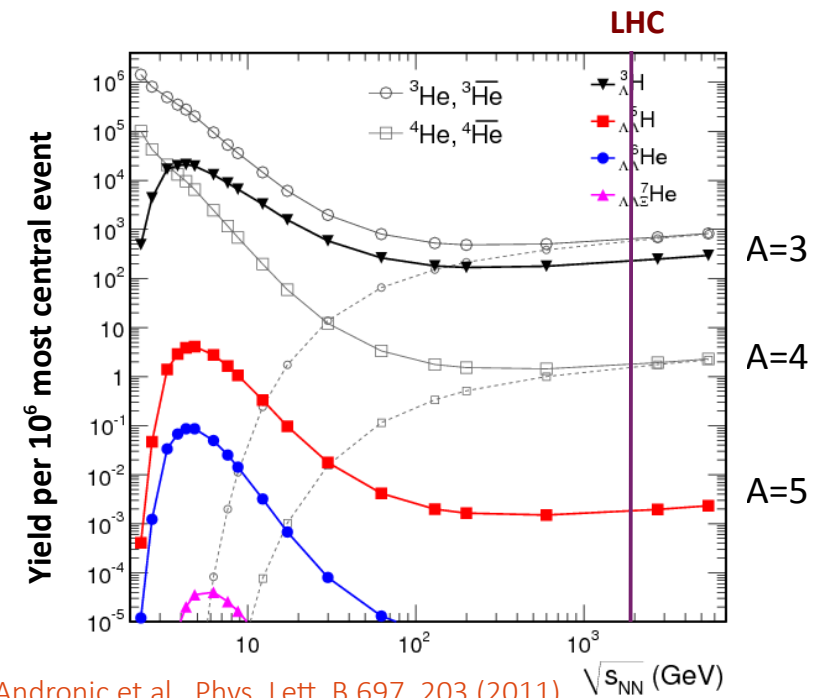
A. Andronic et al., Phys. Lett. B 697, 203 (2011)

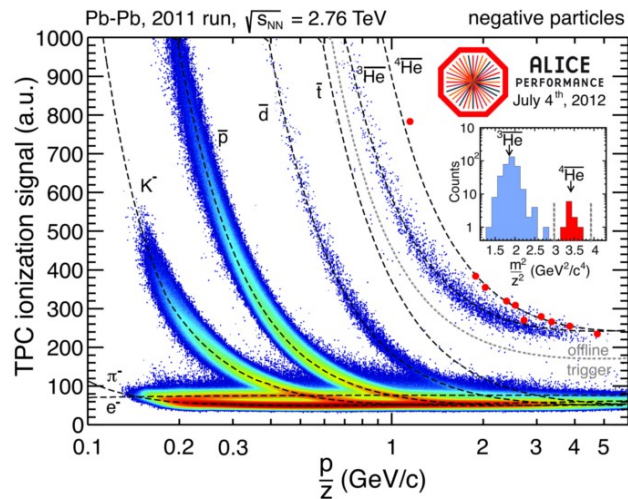# Thermal model fit to ALICE data

The p_T-integrated yields and ratios can be interpreted in terms of statistical (thermal) models

Particle yields of light flavor hadrons (including nuclei) are described with a common chemical freeze-out temperature (T_{chem} = 156 ± 2 MeV)
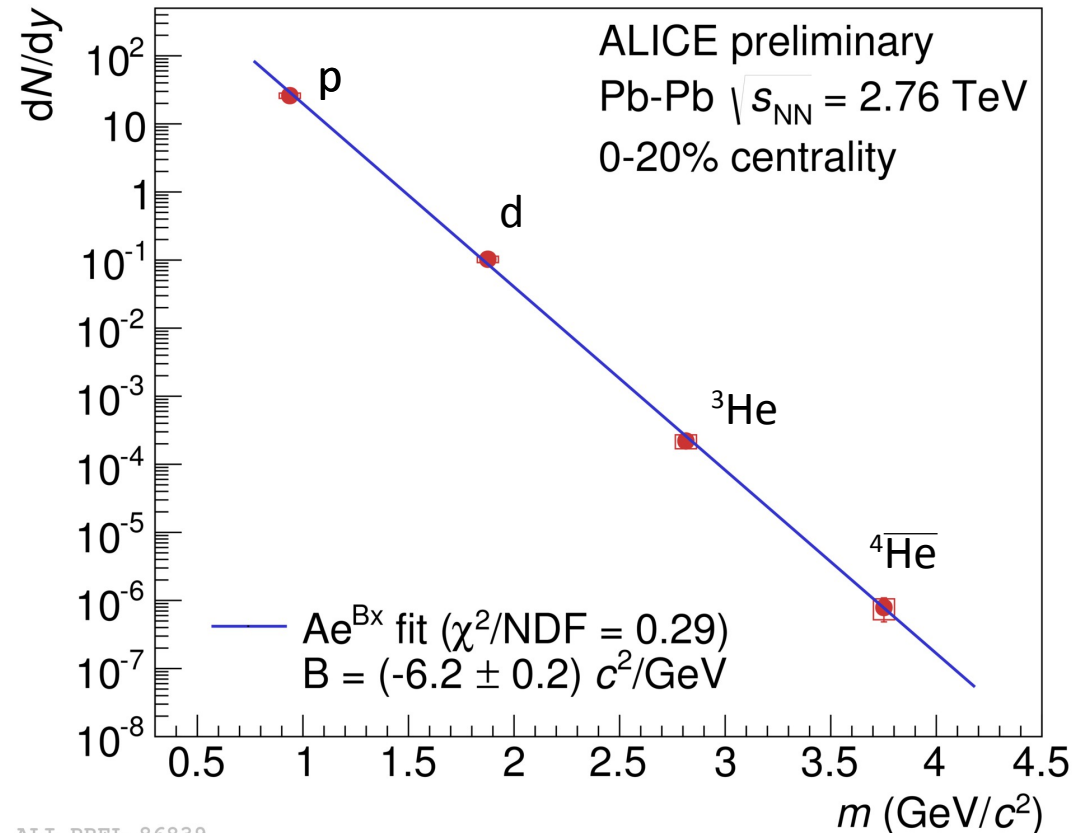
K* not include in the fit

ALI-PREL-75448
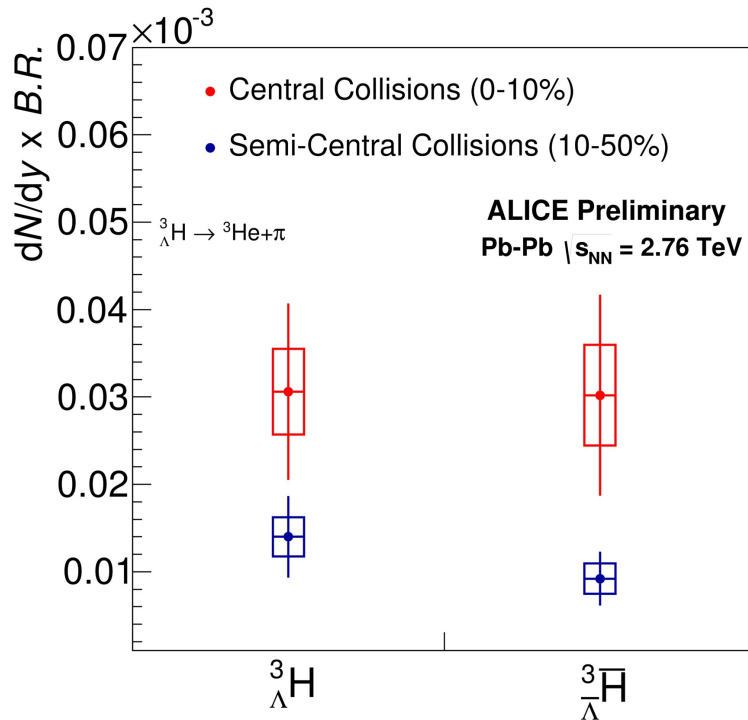
Nuclei in Pb – Pb

Thermal model prediction:

$$\frac{dN}{dy} \propto \exp\left(-\frac{m}{T_{chem}}\right)$$

- Nuclei follow nicely the exponential fall predicted by the model

- Each added baryon gives a factor of ~300 less production yield

ALICE preliminary
Pb-Pb $\sqrt{s_{NN}}$ = 2.76 TeV
0-20% centrality

Ae^{Bx} fit (χ^2/NDF = 0.29)
B = (-6.2 ± 0.2) c^2/GeV

ALI–PREL–86839

$(^3_{\bar{\Lambda}}\overline{H})\ ^3_\Lambda H$ dN/dy

Left plot:
- Central Collisions (0-10%)
- Semi-Central Collisions (10-50%)

$^3_\Lambda H \to {}^3He + \pi$

ALICE Preliminary
Pb-Pb $\sqrt{s_{NN}}$ = 2.76 TeV

$^3_\Lambda H$ $\quad$ $^3_{\bar{\Lambda}}\overline{H}$

ALI-PREL-54275

Right plot:
M. Petran et al. Thermal Model
— T=138.3 MeV, γ_q=1.63, γ_s=2.08

A. Andronic et al. Thermal Model
— T=156 MeV
— T=164 MeV

$^3_\Lambda H \to {}^3He + \pi$

— dN/dy x B.R. - Stat.Error
▯ dN/dy x B.R. - Syst.Error

ALICE Preliminary
Pb-Pb $\sqrt{s_{NN}}$ = 2.76 TeV
Centrality 0-10%

B.R.

ALI-PREL-54321

Yield extracted in two centrality bins
dN/dy in good agreement with thermal
model prediction from Andronic et al. for
T_{chem} = 156 MeV
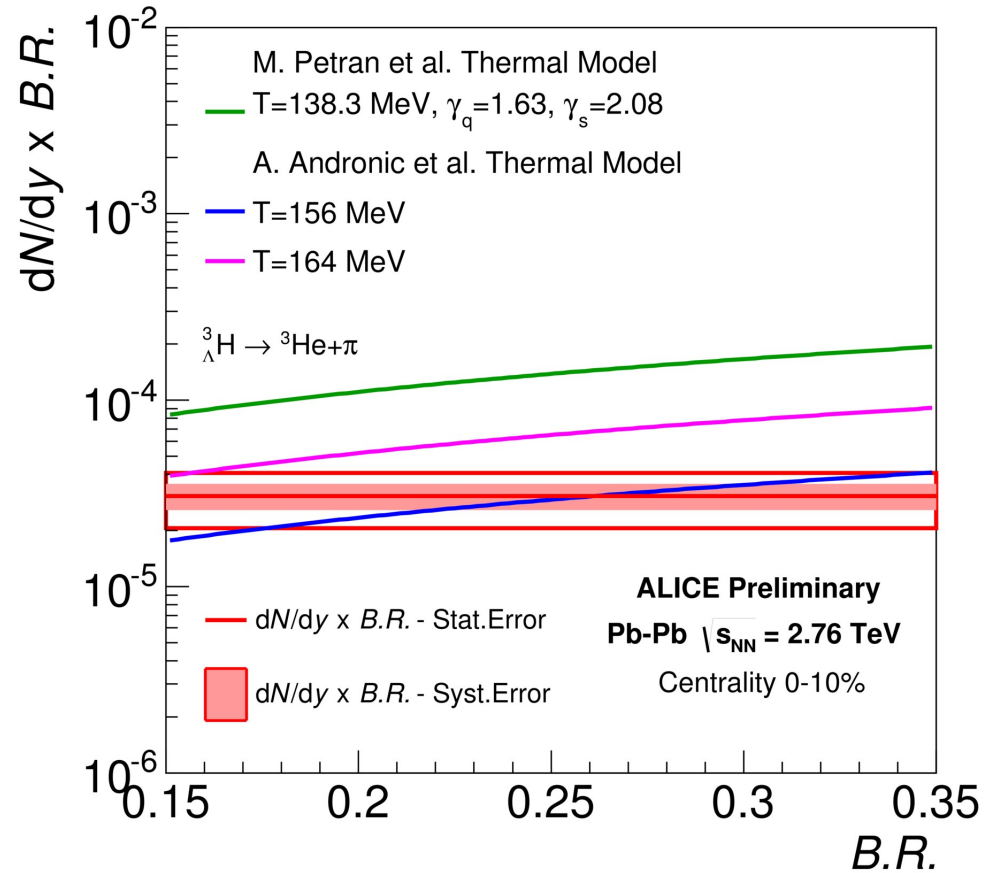
M. Petráň et al., Phys. Rev. C 88, 034907 (2013)
A. Andronic et al., Phys. Lett. B 697, 203 (2011)

Searches for weakly decaying exotic bound states

H-Dibaryon

H-Dibaryon : Hypothetical bound state of *uuddss* (ΛΛ) first predicted by Jaffe in a bag model calculation. Recent lattice calculations suggest a bound state (20-50 MeV/c^2 or 13 MeV/c^2)
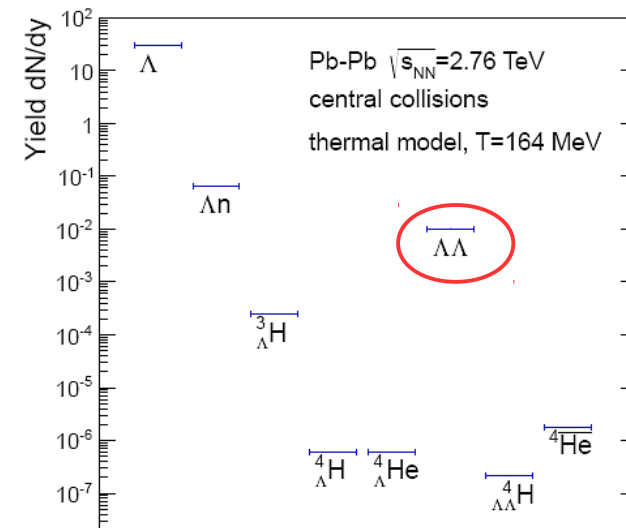
R.L. Jaffe, Phys. Rev. Lett. 38, 195 (1977), erratum ibid 38, 617 (1977)
Inoue et al., PRL 106, 162001 (2011)
Beane et al., PRL 106, 162002 (2011)

If : $m_H <$ ΛΛ threshold

- weakly bound: measurable channel

  H → Λpπ

- 2.2 GeV/$c^2 < m_H <$ 2.231 GeV/c^2
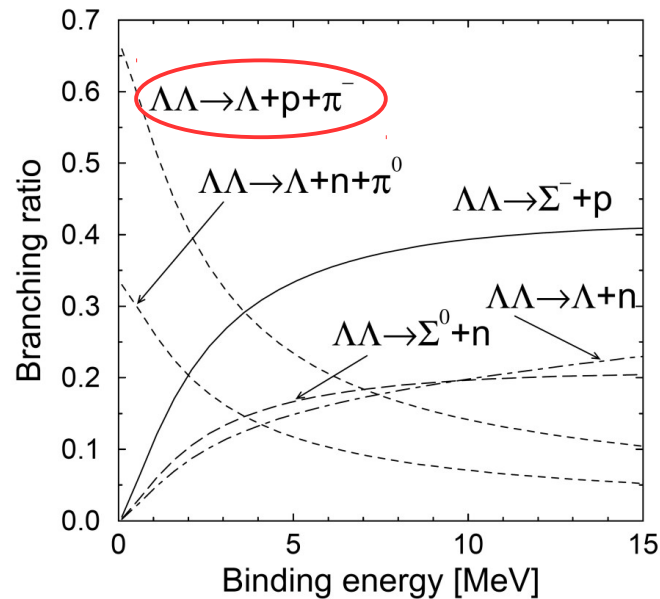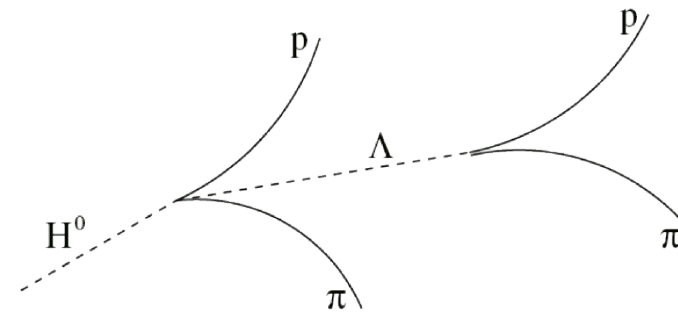
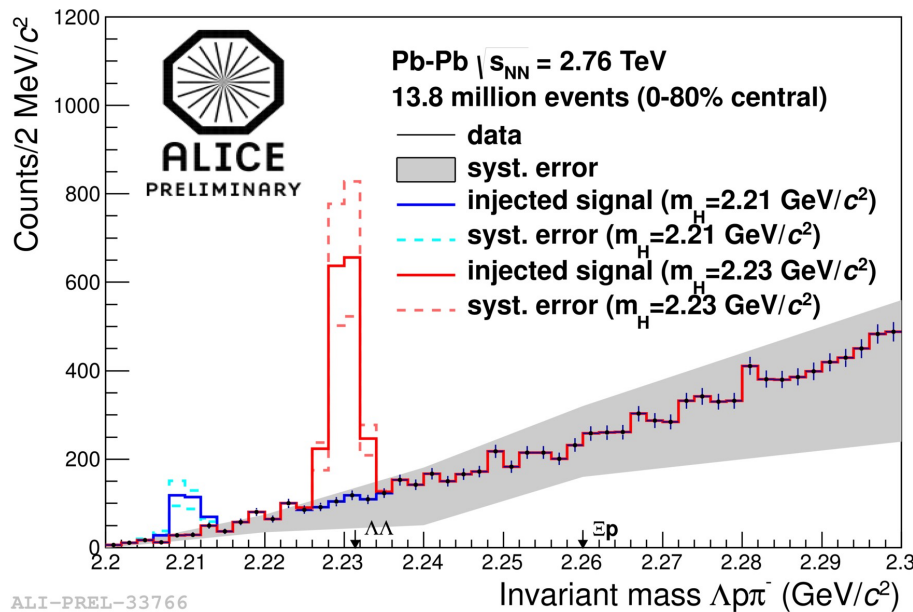Jürgen Schaffner-Bielich et al., PRL 84, 4305 (2000)

A. Andronic, private communication

H-Dibaryon

Expected strongly bound and lightly bound H-Dibaryon signal (thermal model prediction)

$$N = \underbrace{3.1 \cdot 10^{-3}}_{\text{d}N/\text{d}y} \times \underbrace{2}_{y} \times \underbrace{1.38 \cdot 10^{7}}_{\text{events}} \times \underbrace{0.0385}_{\text{Eff.}} \times \underbrace{0.64}_{BR(\Lambda)} = 2110$$

lightly bound:
2110 x 0.64 = 1350

strongly bound:
2110 x 0.1 = 211

Pb-Pb $\sqrt{s_{NN}}$ = 2.76 TeV
13.8 million events (0-80% central)
— data
▓ syst. error
— injected signal (m_H=2.21 GeV/c^2)
- - - syst. error (m_H=2.21 GeV/c^2)
— injected signal (m_H=2.23 GeV/c^2)
- - - syst. error (m_H=2.23 GeV/c^2)

ALI-PREL-33766

No signal visible → upper limits
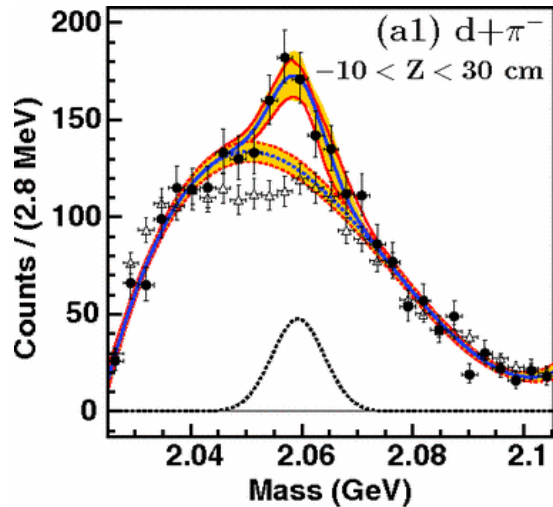
For a lightly bound H:
dN/dy ≤ 2x10^{-4} (99% CL)

For a strongly bound H:
dN/dy ≤ 8.4x10^{-4} (99% CL)

Λn bound state

Bound state of Λn ? HypHI experiment at GSI sees evidence of a new state: Λn → d+ π⁻

C. Rappold et al. (HypHI collaboration), Phys. Rev. C88, 041001(R) (2013)
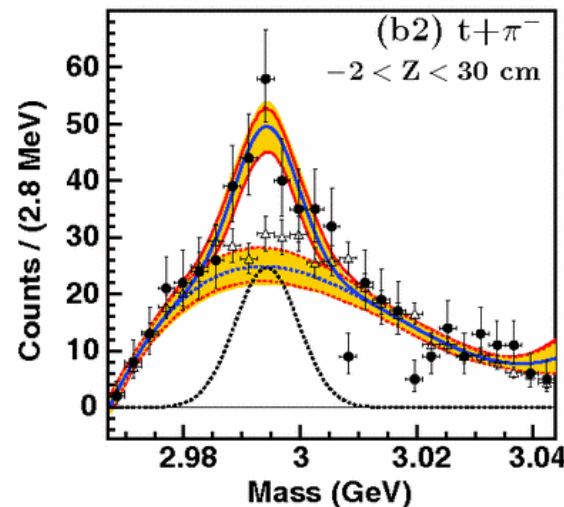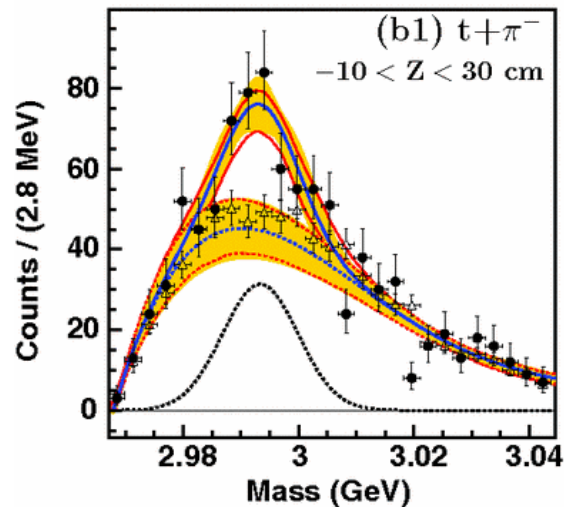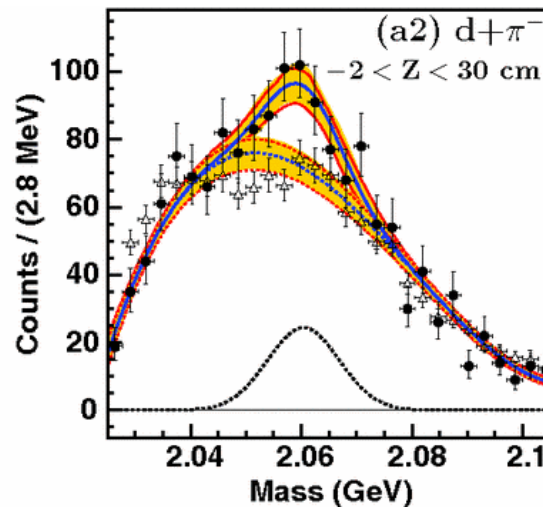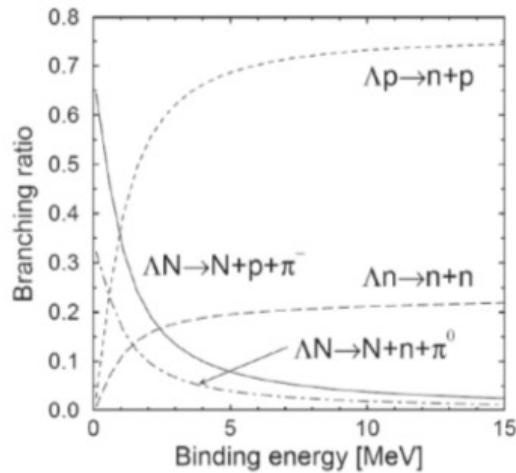

^{6}Li beam at 2 AGeV on ^{12}C target

Experiment intended as hypernuclei factory (search for undiscovered hypernuclei)

Λn bound state

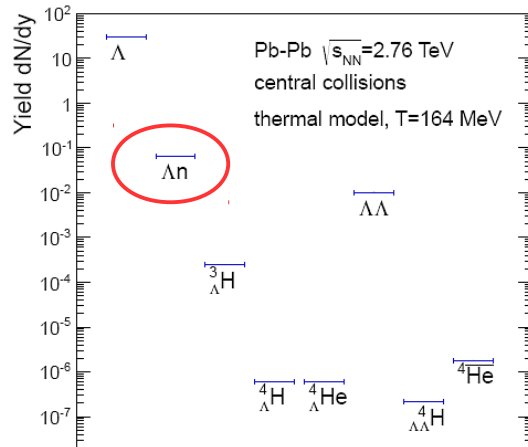Bound state of Λn ? HypHI experiment at GSI sees evidence of a new state: Λn → d+ π⁻

C. Rappold et al. (HypHI collaboration), Phys. Rev. C88, 041001(R) (2013)

Jürgen Schaffner-Bielich, Private communication

A. Andronic, private communication
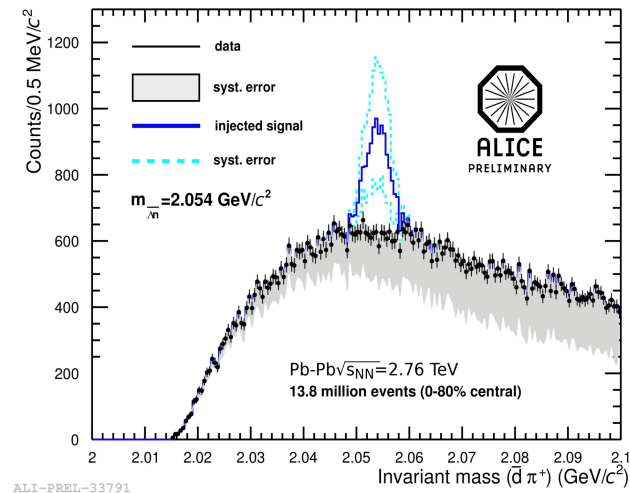
Expected Λn bound states yield at the LHC in (Λn → dπ⁻) (Thermal model prediction):

$$N = \underbrace{1.6 \cdot 10^{-2}}_{dN/dy} \times \underbrace{2}_{y} \times \underbrace{1.38 \cdot 10^{7}}_{events} \times \underbrace{0.0255}_{Eff.} \times \underbrace{0.35}_{BR(Λn)} = 4000$$

No signal visible → upper limit
$dN/dy \leq 1.5 \times 10^{-3}$ (99% CL)
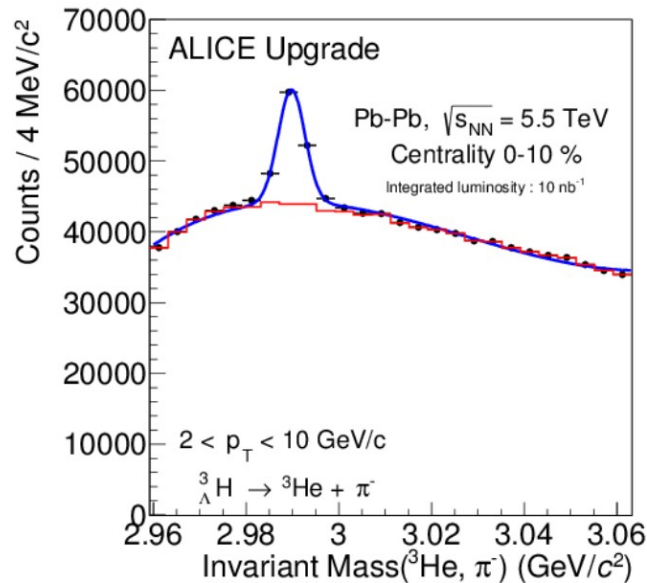
Comparison to different models
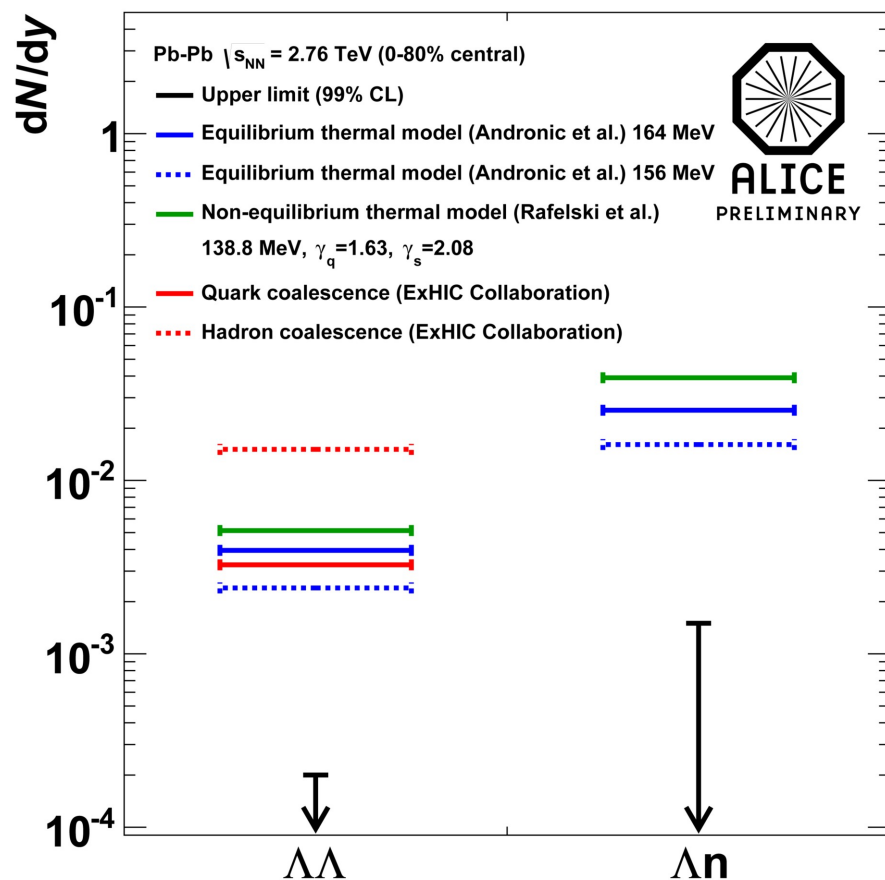
- The upper limits for exotica are lower than the thermal model expectation by a factor 10

- The thermal model with the same temperature describes precisely the production yield of deuterons , ^{3}He and $^3_\Lambda$H

  → At least a factor 10 between models and estimated upper limit

  → The existence of such states with the assumed B.R., mass and lifetime is questionable

Outlook- ALICE Upgrade

After the Upgrade (2018) ALICE will be able to collect data with better performances and higher luminosity.

- Expected integrated luminosity: ~10 nb^{-1} (~ 8×10^9 collisions in the 0-10% centrality class)
- New ITS: less material budget and more precise tracking for the identification of hyper-nuclei
- All the physics which is now done for A = 2 and A = 3 (hyper-)nuclei will be done for A = 4

Expected invariant mass distribution for $^{3}_{\Lambda}$H (plus antiparticle) reconstruction in Pb-Pb collisions (0-10 % centrality class), corresponding to L_{int}= 10 nb^{-1}.

State	dN/dy	B.R.	$\langle Acc \times \varepsilon \rangle$	Yield
$^{3}_{\Lambda}$H	1×10^{-4}	25 %	11 %	44000
$^{4}_{\Lambda}$H	2×10^{-7}	50 %	7 %	110
$^{4}_{\Lambda}$He	2×10^{-7}	32 %	8 %	130

Expected yields for three hypernuclear states (plus their antiparticles) for central Pb-Pb collisions (0-10 %) at $\sqrt{s}_{NN}$ = 5.5 TeV

Technical Design Report for the Upgrade of the ALICE Inner Tracking System
B. Abelev et al. (The ALICE Collaboration) 2014 J. Phys. G: Nucl. Part. Phys. 41 087002

Conclusions

- Excellent ALICE performance allows detection of light (anti-)nuclei, (anti-)hypernuclei and other exotic bound states

- A hardening of the deuteron and ^{3}He spectra with increasing centrality is observed both in Pb-Pb and p-Pb collisions

- The d/p ratio rises with multiplicity in p-Pb collisions, while no significant centrality dependence is observed in Pb-Pb collisions

- Coalescence parameter B_2 is independent from p_T in p-Pb and peripheral Pb-Pb collisions, while it increases with p_T in central Pb-Pb collisions. These two observations are consistent with a coalescence model where B_2 scales like HBT radii

- The measured $^3_\Lambda$H lifetime (185 ± 48 ± 29 ps) is consistent with previous measurements

- Measured deuteron, ^{3}He, hypertriton and anti-alpha yields are in agreement with the current best thermal fit from equilibrium thermal model (T_{chem} = 156 MeV)

- H-Dibaryon and Λn search in Pb-Pb with ALICE: no visible signal → Upper limits are at least an order of magnitude lower than predictions of several models
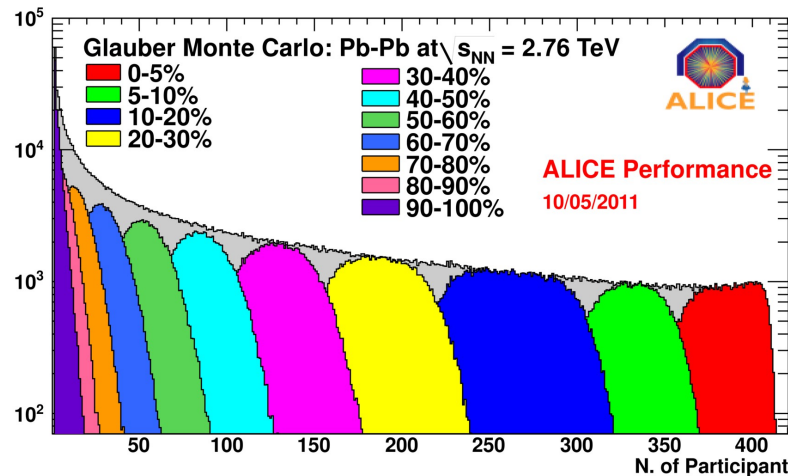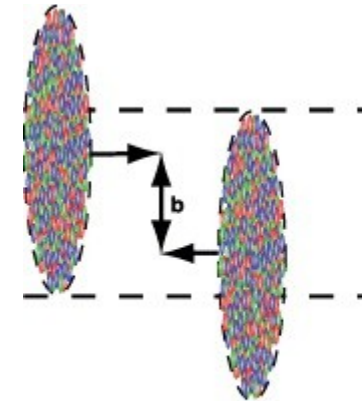
BACKUP

Collision Geometry

Centrality = degree of overlap of the 2 colliding nuclei

Central collisions:
- small impact parameter b
- high number of participant nucleons → high multiplicity

Peripheral collisions:
- large impact parameter b
- low number of participant nucleons → low multiplicity

Glauber Monte Carlo: Pb-Pb at $\sqrt{s_{NN}}$ = 2.76 TeV

0-5%	30-40%
5-10%	40-50%
10-20%	50-60%
20-30%	60-70%
	70-80%
	80-90%
	90-100%

ALICE Performance
10/05/2011

N. of Participant

Geometrical picture of AA collisions with the Glauber model:

- Random relative position of nuclei in transverse plane Woods-Saxon distribution of nucleons inside nucleus
- Straight-line nucleon trajectories
- N-N cross-section (s_{NN} = 64 ± 5 mb)

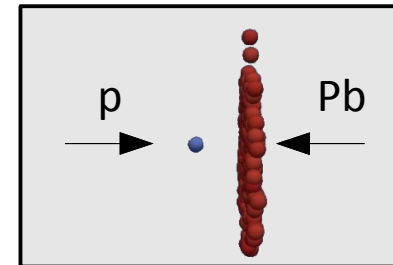independent of the number of collisions the nucleons suffered before

Centrality in p − Pb

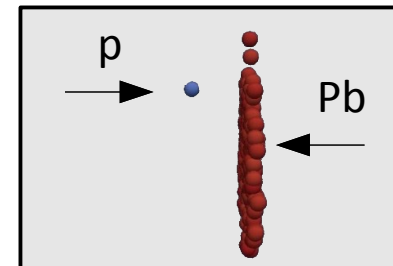Multiplicity estimator: slices in VZERO-A (V0A) amplitude
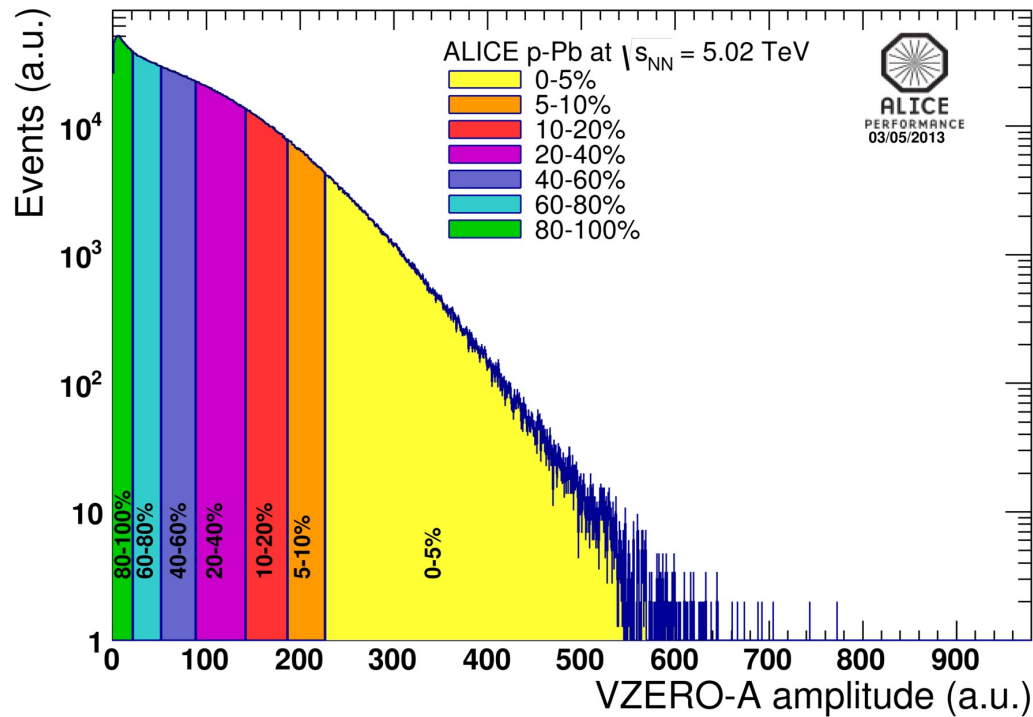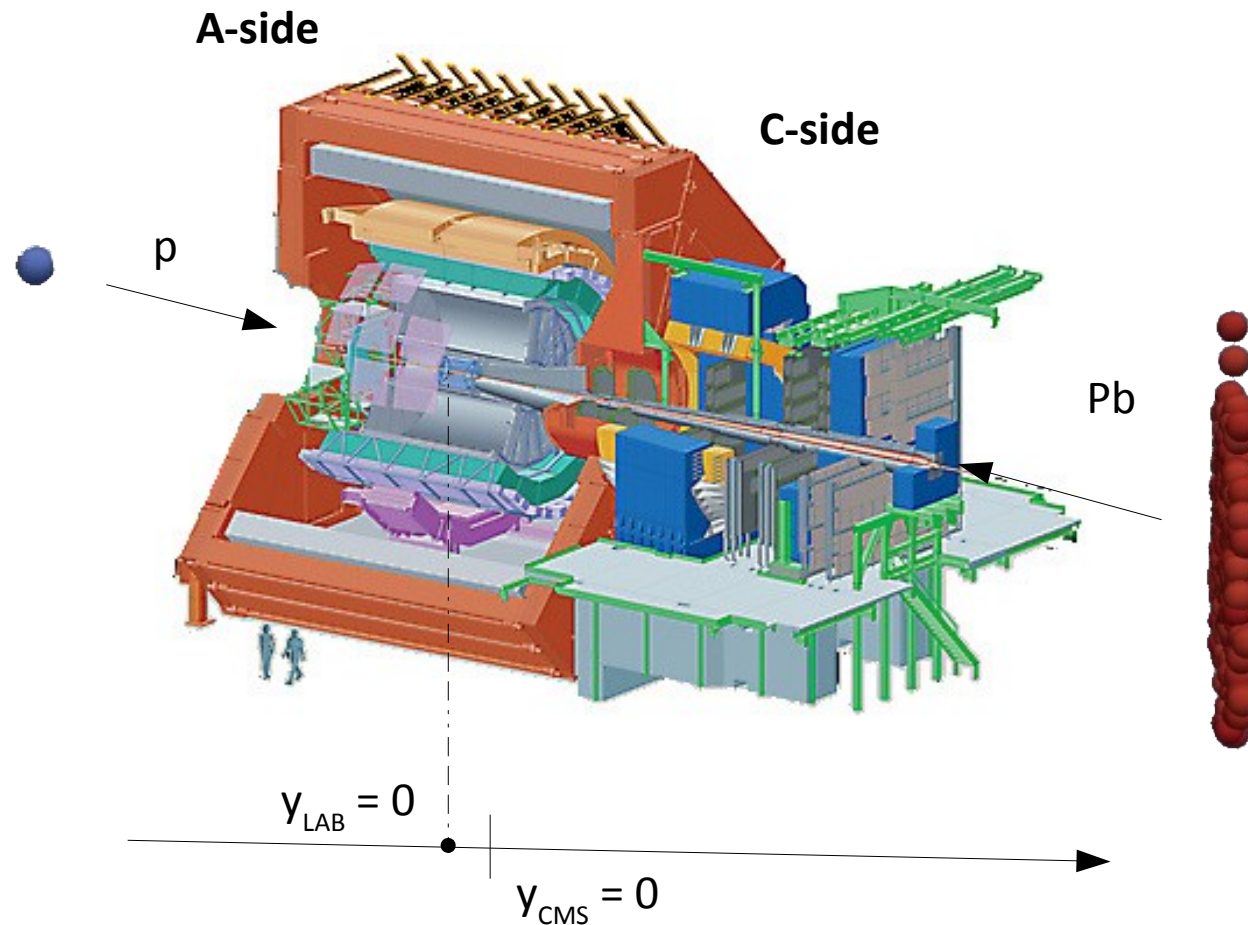

ALI−PERF−51387

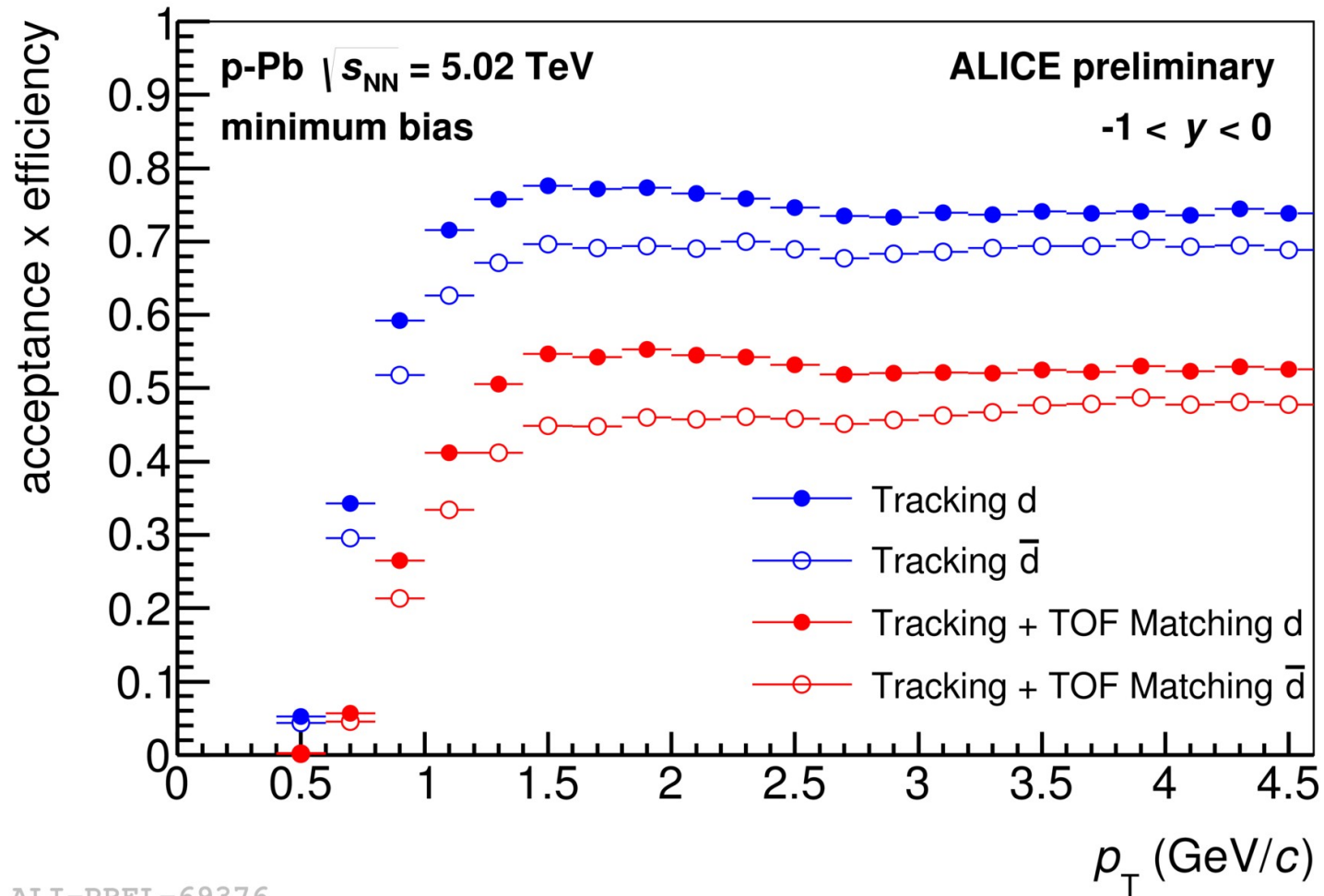Central collision

Peripheral collision

Correlation between impact parameter and multiplicity is not as straight-forward as in Pb-Pb

Rapidity definition in p − Pb

Asymmetric energy/nucleon in the two beams → CMS moves with rapidity $|\Delta y_{CMS}| = 0.465$
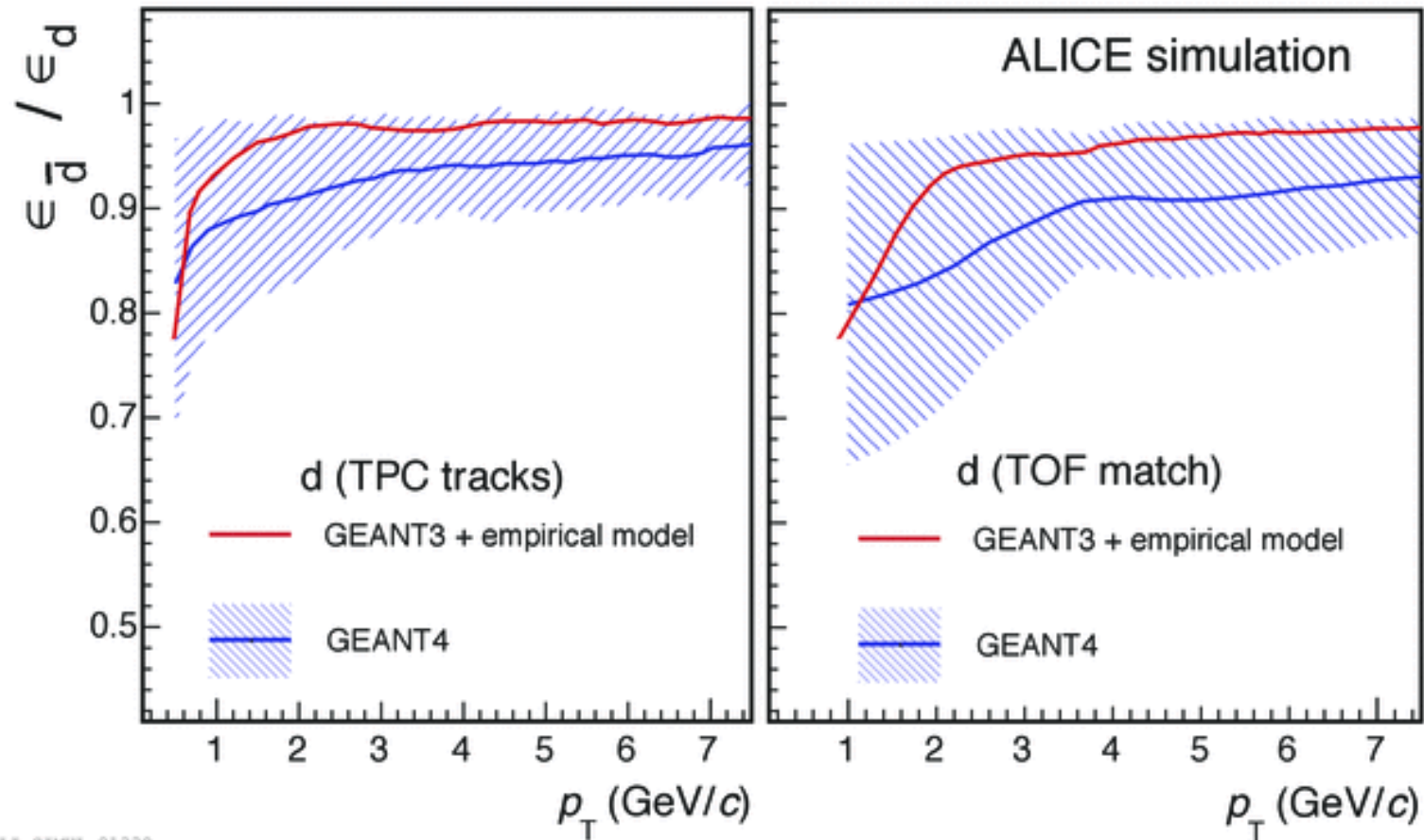
Efficiency Correction

ALI-PREL-69376

Absorption Correction

ALI-SIMUL-81330

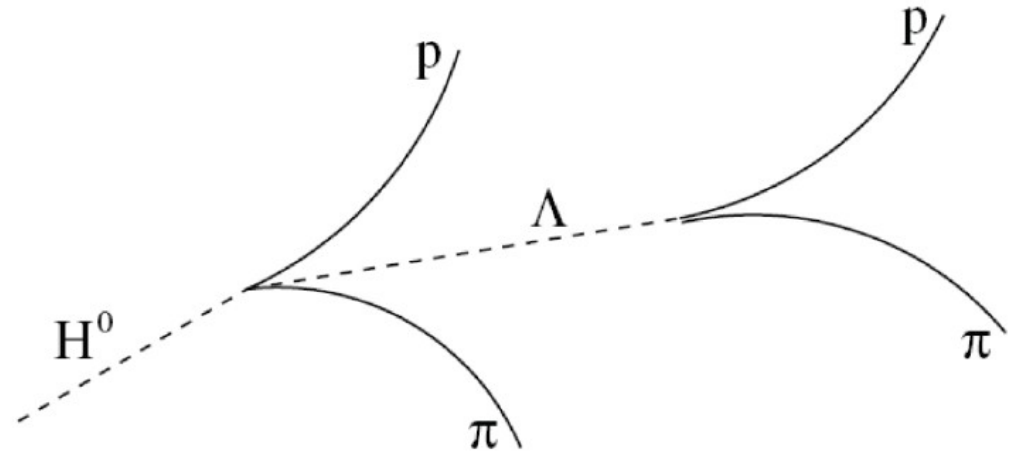For the anti-deuteron spectra an additional correction is necessary due to the absorption

H-Dibaryon

Two cases:

- $m_H < \Lambda\Lambda$ threshold

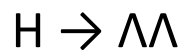 - weakly bound:
    measurable channel
    $$H \to \Lambda p\pi$$

  - 2.2 GeV/c^2 < m_H < 2.231 GeV/c^2

- $m_H > \Lambda\Lambda$ threshold

  - resonant state:
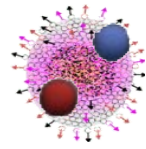   measurable channel
    $$H \to \Lambda\Lambda$$
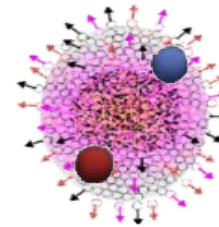
  - m_H > 2.231 GeV/c^2
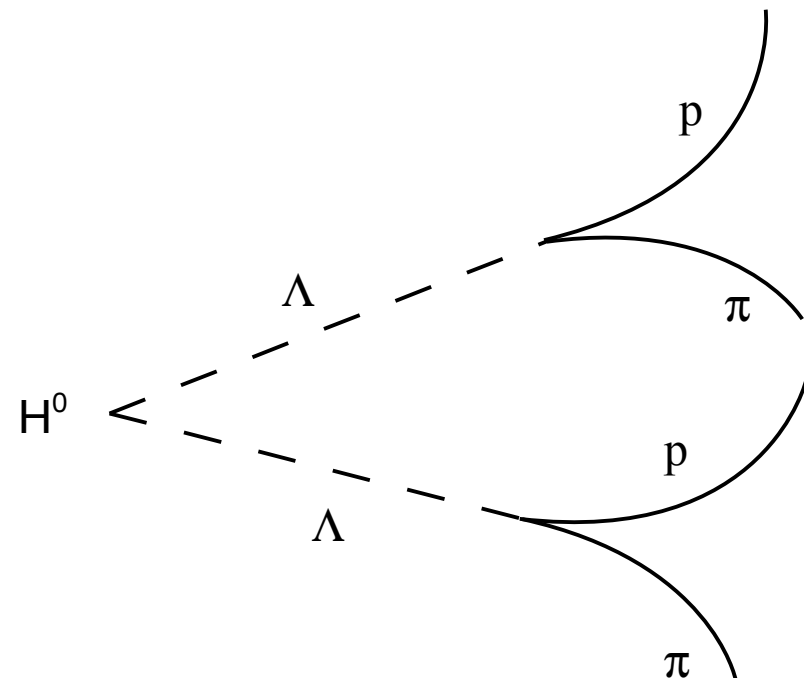
Coalescence Model and HBT

The size of the emitting volume (V_{eff}) has to be taken into account: the larger the distance between the protons and neutrons which are created in the collision, the less likely is that they coalesce

(small fireball)

(large fireball)

In detail, it turns out [1] that the coalescence process is governed by the same "length of homogeneity in the source" which can be extracted from two particle Bose-Einstein correlation (HanburyBrown – Twiss (HBT) interferometry [2]): $\rightarrow B_2 \sim 1/V_{eff}$

$$B_2 = \frac{3\pi^{3/2}\langle C_d \rangle}{2 m_t \Re_T^2(m_t) \Re_p^2(m_t)} e^{2(m_t - m)\left(\frac{1}{T^* p} - \frac{1}{T^* d}\right)}$$

The strong decrease of B_2 with centrality in Pb-Pb collisions can be naturally explained as an increase in the emitting volume: particle densities are relevant and not absolute multiplicities

[1]R. Scheibl and U. Heinz, Phys.Rev. C59, 1585 (1999)
[2]A review can be found in : U. Heinz, Nucl. Phys. A 610 , 264c (1996)